NCAT Report 03-03

WORKABILITY OF HOT MIX ASPHALT

By

Jagan M. Gudimettla
L. Allen Cooley, Jr.
E. Ray Brown

April 2003

National Center for Asphalt Technology
NCAT
AUBURN UNIVERSITY
277 Technology Parkway Auburn, AL 36830

WORKABILITY OF HOT MIX ASPHALT

By:

Jagan M. Gudimettla
Graduate Student
National Center for Asphalt Technology
Auburn University, Auburn, Alabama

L. Allen Cooley, Jr.
Manager, Southeastern Superpave Center
National Center for Asphalt Technology
Auburn University, Auburn, Alabama

E. Ray Brown
Director
National Center for Asphalt Technology
Auburn University, Auburn, Alabama

NCAT Report 03-03

April 2003

DISCLAIMER

The contents of this report reflect the views of the authors who are responsible for the facts and accuracy of the data presented herein. The contents do not necessarily reflect the official views or policies of the National Center for Asphalt Technology or Auburn University. This report does not constitute a standard, specification, or regulation.

TABLE OF CONTENTS

ABSTRACT

The term workability has been used to describe several properties related to the construction of hot mix asphalt (HMA). Workability in the field can be defined as a property that describes the ease with which a HMA can be placed, worked by hand, and compacted. This definition provides a term that is applicable to movement of HMA through equipment to the roadway, handwork of HMA, and compactibility on the roadway.

Due to the performance benefits of polymer-modified binders, their use has increased in the US. However, with the use of polymer-modified binders, the workability of HMA decreases substantially at a given temperature since the modifiers tend to increase the viscosity of binders. Compacting HMA with polymer-modified binders can be more difficult with modified binders than for mixes that utilize unmodified binders. If the compositional properties of a mix, such as aggregate physical properties and gradation are kept constant, workability of HMA is basically a function of binder properties at a given temperature. The higher the temperature the better is the mix workability since the viscosity of the binder decreases as temperature increases. However, increasing the mix temperature to obtain a desired workability is not always best. Problems that result from excessive temperature include: 1) damage to asphalt (heat hardening); 2) damage to additives; 3) increased fuel consumption; and 4) increased smoke and volatile organic compounds (VOC) production.

The primary objective of this study was to develop a device to measure the workability of HMA mixes that could identify the change in workability due to changes in mix characteristics. Secondly, this study was to evaluate a method in which mix workability could be used for establishing approximate compaction temperatures for HMA mixes.

Based on the findings of this study a device was successfully designed to measure the laboratory workability of HMA mixes. The device immerses a paddle into a sample of HMA. The torque required to keep the paddle rotating at a constant speed within the sample is then measured. Workability was defined as the inverse of the torque required to rotate the paddle within the sample of HMA. The workability of HMA was affected by aggregate type, and, thus, aggregate properties. Mixes prepared with a cubical, angular granite were less workable (generated more torque at a given temperature) than mixes prepared with a semi-angular crushed gravel. The workability of HMA was affected by the nominal maximum aggregate size (NMAS) of the gradation. As NMAS increased for a given aggregate type, gradation shape, and binder type, workability decreased. Gradation shape did not have a significant effect on workability. However, there were numerous two- and three-way interactions that were significant that included gradation shape. Binder type significantly affected the workability of mixes. Mixes modified to meet a PG 76-22 were significantly less workable than mixes containing an unmodified PG 64-22. There was a relationship between workability and temperature that showed increased workability at higher temperatures. A preliminary attempt was made at utilizing workability data to determine a realistic compaction temperature of HMA mixes. However, this was a limited effort and the results were inconclusive.

WORKABILITY OF HOT MIX ASPHALT

Jagan M. Gudimettla, L. Allen Cooley, Jr., and E. Ray Brown

INTRODUCTION

The term workability has been used to describe several properties related to the construction of hot mix asphalt (HMA). First, some have used this term to describe the ease with which HMA can be worked by hand after being placed on the roadway. Others have also used the term workability to describe the compactibility of HMA. In combination, workability can be defined as a property that describes the ease with which a HMA can be placed, worked by hand, and compacted. This definition provides a term that is applicable to movement of HMA through construction equipment to the roadway, handwork of HMA, and compactibility on the roadway.

Satisfactory workability is important in obtaining the desired HMA smoothness and density within a compacted pavement. For mixtures that are very harsh, therefore having low workability, it can be more difficult to construct smooth pavements. Pavements that are under-compacted may experience significant performance problems primarily due to high voids *(1).* If not properly compacted, the potential for permeability problems, as well as rate of oxidative aging of the binder, is increased considerably thereby reducing the life of the pavement.

Due to the performance attributes of polymer-modified binders, their use has increased in the US. However, with the use of polymer-modified binders, the workability of HMA decreases substantially at a given temperature since the modifiers tend to increase the viscosity of binders. Therefore, compacting HMA to achieve the desired density can be more difficult with modified binders than for mixes that utilize unmodified binders. If the compositional properties of a mix, such as aggregate physical properties and gradation are kept constant, workability of HMA is basically a function of binder properties at a given temperature. The higher the temperature the better is the mix workability since the viscosity of the binder decreases as temperature increases. However, increasing the mix temperature to obtain a desired workability is not always best. Problems that result from excessive temperature include: 1) damage to asphalt (heat hardening); 2) damage to additives; 3) increased fuel consumption; and 4) increased smoke and volatile organic compounds (VOC) production *(2, 3).*

Traditionally, binder viscosity has been used to determine mixing and compaction temperatures of HMA. Compaction temperatures obtained with this method directly affect the workability of the mix since equi-viscous binder conditions are used. But with the increasing use of modifiers and new HMA mix types (e.g., Superpave and stone matrix asphalt), problems with selecting satisfactory mixing and compaction temperature have been observed. Therefore, a study was needed to assess methods of evaluating the workability of HMA mixtures and the use of workability to establish mixing and compaction temperatures needs to be evaluated.

Objective

The primary objective of this study was to develop a device to measure the workability of HMA mixes that can identify the change in workability due to changes in mix characteristics. Secondly, this study was to evaluate a method in which mix workability could be used for establishing approximate compaction temperatures for HMA mixes.

Scope

A literature review was conducted to identify developments in measuring the workability of HMA and other materials. This information was used to develop a device to measure the workability of HMA mixes. Initial tests with the fabricated device included testing of mixes having different expected ranges of workability to evaluate any equipment limitations so that necessary modifications could be made. Once modifications were made, further testing was conducted to optimize the equipment configuration. After the equipment configuration was finalized, mixes with different combinations of binders, aggregates, gradation shape and nominal maximum aggregate size (NMAS) were evaluated with the device. This data was then analyzed to determine the effect of individual mix constituents on the workability of HMA. Workability data of mixes with the same combinations of gradation, aggregate properties, and nominal maximum aggregate size, but with different binders, were also evaluated to potentially propose a preliminary method for establishing the compaction temperature for HMA mixes. A Superpave gyratory compactor (SGC) equipped to measure the gyratory shear was used to evaluate this preliminary method of establishing compaction temperature.

BACKGROUND AND PROBLEM STATEMENT

Within this section, a review of literature on methods of measuring the workability of HMA is provided. Also included within this section is a discussion on why the measurement of HMA workability is important. Most specifically, the effect of polymer modified versus unmodified binders is discussed. Finally, current methods of determining the mixing and compaction temperatures for HMA are discussed.

Literature Review on Measuring Workability

An attempt at measuring the workability of HMA was presented at AAPT in 1978 by Marvillet and Bougault *(4).* According to the paper, workability of HMA is dependent on the composition of the mixture, such as binder grade, amount of binder, and aggregate properties (type, gradation, etc). The authors also found workability dependent on external parameters such as the design of the equipment and temperature.

Marvillet and Bougault described an instrument that can measure the workability of HMA. The instrument (Figure 1) consisted of a chamber that is attached to a rigid frame. A motor, mounted on top of the frame, rotates a single blade within the mix at a constant rotational speed. The total weight of the mix used by the authors was approximately 15 kilograms. A spring, along with a potentiomer, was attached to the rigid frame of the machine and was used to measure the resistance of mix within the chamber against the rotation of the blade. The electrical signal was converted to numeric values and expressed in units of torque.

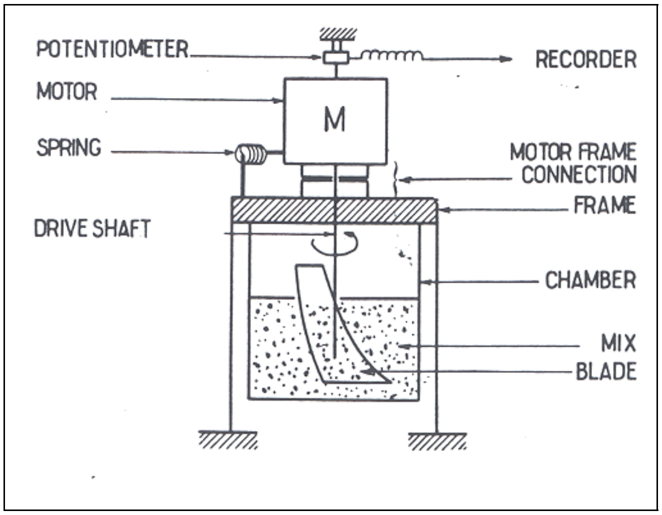

Figure 1. Diagram of the Workability Meter *(4)*

A CORECI regulator was used for measuring and displaying the temperature of the mix. The entire chamber where the mix was placed was heated to raise the temperature of the mix at the rate of 1°C/min. Test results were recorded as the temperature increased from 150°C to 200°C. The blade used to push the mix rotated at a constant rotational speed of 22 RPM. In Marvillet and Bougalt's paper, the term "Workability" was defined as the inverse of the resistance moment (torque) produced by the mix against the rotation of the blade. Therefore, as torque increased, workability decreased.

Results from Marvillet and Bougalt`s study *(4)* can be summarized as follows:

- Workability of HMA mixtures increased as the viscosity of the binder grade decreased.
- Change in binder content did not have any direct relationship with workability.
- As the filler content in the mix increased, the workability decreased.
- Mixes with angular particles were less workable than mixes having semi-angular or round aggregate particles.

A number of devices have been used to measure the workability of Portland cement concrete. One device is the two-point workability device *(5)*. In the Two-point workability device the torque required to rotate an impeller at a constant speed while submerged in the concrete is measured. The impeller, or paddle, is rotated at various speeds and the corresponding values of torque are noted. The Two-point workability machine is illustrated in the Figure 2.

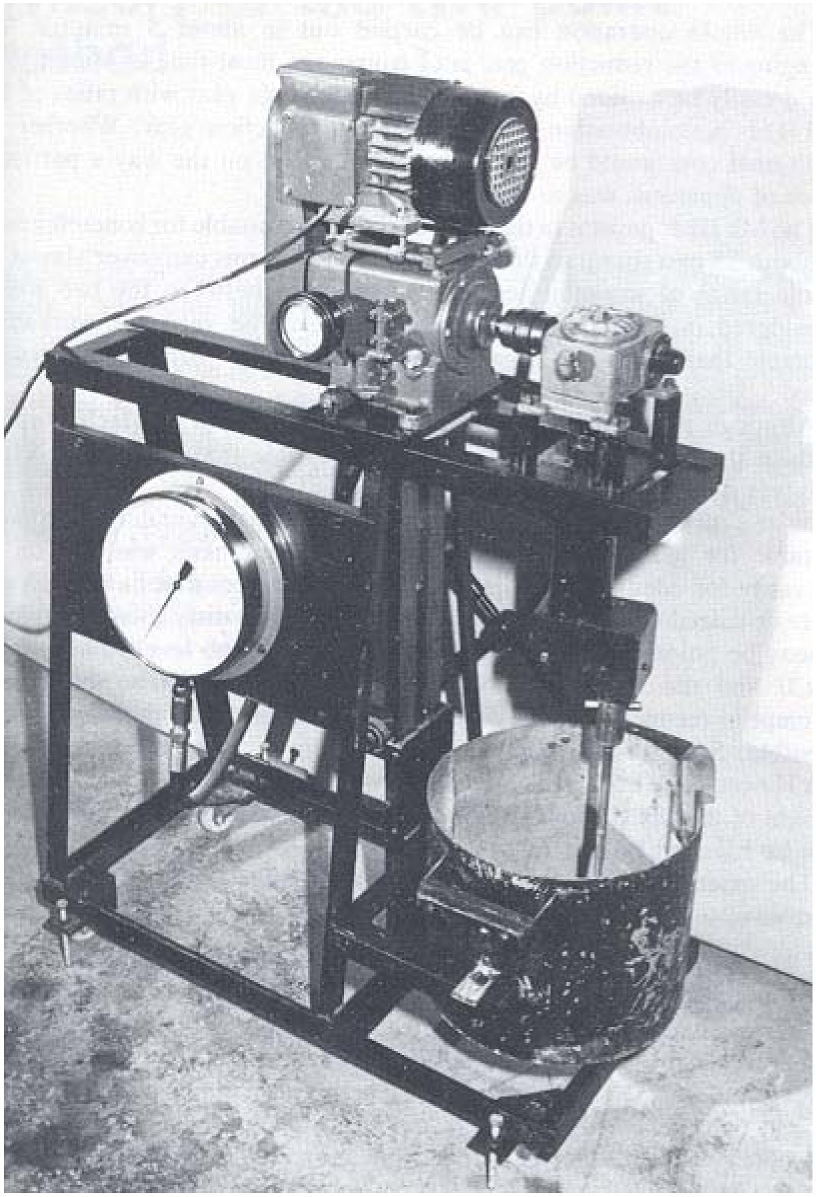

Figure 2. Two-Point Workability Machine *(5)*

Need for Measuring Workability of HMA

Modification of asphalt binders has increased within the last few years. Modifiers have increased the resistance of HMA pavements to some major distresses such as deformation (rutting), cracking (thermal and fatigue) and disintegration (raveling and stripping). Several laboratory studies, as well as field experience, have shown the effectiveness of using modified binders in HMA. According to Terrel and Epps *(3)*, some of the reasons for modification are:

- Reduced
    1. Structural thickness of pavement layers.
    2. Life cycle cost of pavement.
    3. Low temperature cracking of pavements.

- Improved
  1. Fatigue resistance of asphalts.
  2. Bonding between aggregate and asphalt and thus reduce stripping.
  3. Resistance to aging or oxidation.
  4. Crack sealing.
  5. Overall performance of pavements.
  6. Strength and stability of mixes.

The different types of additives commonly used as HMA modifiers based on generic classifications, according to Terrel and Epps, are shown in Table 1. Each type of modifier shown in the table has a specific use. For example mineral fillers, extenders, rubbers, plastics, fibers, oxidants and hydrocarbons are often helpful in increasing the stiffness of the pavement at higher temperatures and reducing stiffness at lower temperatures *(3).* Modifiers like lime can be used to improve the adhesion between asphalt and aggregate in the presence of water, thereby, reducing the stripping potential in HMA. Some mineral fillers, antioxidants and hydrocarbons can improve the binder's long-term durability.

Table1. Generic Classification of Binder Modifiers *(3)*

Type	Examples
Filler	Mineral filler, Carbon Black, Sulphur
Extender	Sulphur, Lignin
Polymers	Rubber, Plastic
Fiber	Natural, Man made
Oxidant	Manganese Salt
Antioxidant	Carbon, Calcium Salts
Hydrocarbon	Recycling and Rejuvenating oils
Antistrip	Amines and Lime

Along with the advantages associated with modified binders there are problems as well, most of which are construction-related. These include identification of appropriate mixing and compaction temperatures, pumpability of the modified binders, and short and long-term aging of HMA. A paper published in the Association of Asphalt Paving Technologists (AAPT) titled "Classification of Asphalt Binders into Simple and Complex Binders" *(6)* reported the results of a survey describing problems encountered with the viscosity-temperature method for determining mixing and compaction temperatures for modified binders. The most frequent problem being that mixing and compaction temperatures obtained by the traditional temperature-viscosity method for modified asphalt binders were much higher than those for unmodified binders.

The problems associated with high compaction temperatures are many. As noted, asphalt binders are mixed with modifiers to achieve specific qualities. When modified binders are heated to high temperatures separation may take place between the modifier and base asphalt *(7).* If this happens the effectiveness of the modified binder will be reduced. There are several other problems as well, some of which include:

- Excessive heating may result in oxidation of the binder, and damage which may result in premature pavement cracking.
- Both visible (smoke) and non-visible emissions increase as the binder's temperature is increased. This may pose health and environmental problems.
- Due to separation, modifiers may be extruded from the mix onto the pavement surface under breakdown rolling. This will cause excessive pick-up of material when using rubber tire rollers, which may cause unacceptable surface texture.
- Heating the HMA mix to a high temperature can also release the internal moisture of the aggregates. The moisture can then cause the binder to be semi-emulsified during the vibratory rolling process, which may lead to tenderness.
- Also excessive compaction temperatures can mean excessive mixing temperature. This may cause draindown of the binder in haul trucks for mixes like SMA (Stone Matrix Asphalt) and OGFC (open-graded friction courses) that use high asphalt contents.

During the 1990s, there were some major advances in the design of HMA mixes. Mix design systems for Superpave and Stone Matrix Asphalt (SMA) were adopted in the U.S. Both of these design systems have proven to reduce the amount of rutting on the nation's highways *(8).* However, with these new mix design systems came a wider range in gradations than used in the past. Historically, gradations associated with both the Marshall and Hveem mix design systems passed close to or above the maximum density line. Gradations within the Superpave system are allowed to pass either above or below the maximum density line. SMA mixes are very coarse and generally contain 70 to 80 percent coarse aggregate (retained on 4.75 mm sieve). It would be expected that mixes containing the same aggregate and binder type, but having different gradations will likely have different workabilities.

Determining Mixing and Compaction Temperatures

The equi-viscous temperature range of asphalt has long been used in establishing the mixing and compaction temperatures for mix designs and field production. This procedure assumes that two mixes with the same aggregate gradation exhibit similar volumetric properties when mixed with soft or hard binder as long as they are mixed when the asphalt viscosity is similar.

The Asphalt Institute presented the first recommendation for the laboratory mixing and compaction temperature ranges based on viscosity of asphalt in 1962 within its publication "Mix Design Methods for Asphalt Concrete and Other Hot-mix Types" *(9).* According to this method the temperature to which asphalt must be heated to produce viscosities of 85±10 seconds Saybolt-Furol and 140±15 seconds Saybolt-Furol should be taken as mixing and compaction temperature, respectively. Saybolt-Furol viscosity is the viscosity of a liquid measured based on the time taken for a specific amount of liquid to flow through an orifice of specified dimensions. In 1974, the Asphalt Institute changed the viscosity measurements from units of Saybolt-Furol to units of centistokes (cSt) *(10).* In this procedure absolute viscosity, in poise, at 60°C and kinematic viscosity at 135°C in cSt are measured. The absolute viscosity at 60°C is then converted into kinematic viscosity (cSt) by dividing viscosity by the specific gravity of the binder at 60°C. The two kinematic viscosity points are then plotted on a viscosity and temperature graph with viscosity on a log-log centistokes scale and temperature in log Rankine. The two points are joined as a straight line. Once the line is established, viscosity ranges of 170±20 cSt were recommended for mixing temperature and 280±30 cSt for compaction temperature, while performing the Marshall mix design.

With Superpave, the basic concept of equi-viscous mixing and compaction remained the same. However, the units of measuring viscosity changed from cSt to Pascal-seconds (Pa-s) and the viscosity values are now determined using a Rotational Viscometer at 135°C and 165°C. Once the two points on a semi-log graph are known the temperature-viscosity relationship is established. After this line is established on the graph the viscosity range of 0.17±0.02 Pa-s is used for mixing temperature and 0.28±.03 Pa-s is used for compaction temperatures during Superpave mix design (Figure 3).

As can be seen from all the procedures described above, the basic principles remain that both mixing and compaction temperatures should be taken as the temperature at which the binder achieves a specific viscosity. Using this concept, polymer-modified binders require much higher temperatures to attain the same viscosity as unmodified binders. Temperatures obtained for mixing and compaction by the existing methods can be 177° C or higher. This is not reasonable based on experience.

Recently, Yildrim et al. *(11),* put forth a new method for determination of mixing and compaction temperature. According to this paper the traditional method of using viscosity and temperature to determine the mixing and compaction temperature is suited for unmodified binder but not for modified binders. The authors indicate that unmodified binders are basically Newtonian in nature; that is their viscosity is not shear rate dependent. Modified binders at certain temperatures tend to exhibit a property called shear thinning, or pseudo-plasticity, where viscosity depends on shear rate. They suggested that shear rate inside the rotational viscometer does not simulate the shear rates inside a gyratory compactor during compaction. The paper concludes that the shear rate inside the Superpave gyratory compactor should be calculated first and then points on the temperature-viscosity graph should be obtained by measuring the viscosity at those shear rates. Once the two points are obtained the paper says that the viscosity-temperature graph can be used to determine the mixing and compaction temperatures.

De Sombre et al. *(12)* also provide an idea on the compaction temperature range for HMA. The author considered the asphalt mix to behave similar to a soil, and used Mohrs-Columb equation to explain the shear stress in the HMA mix:

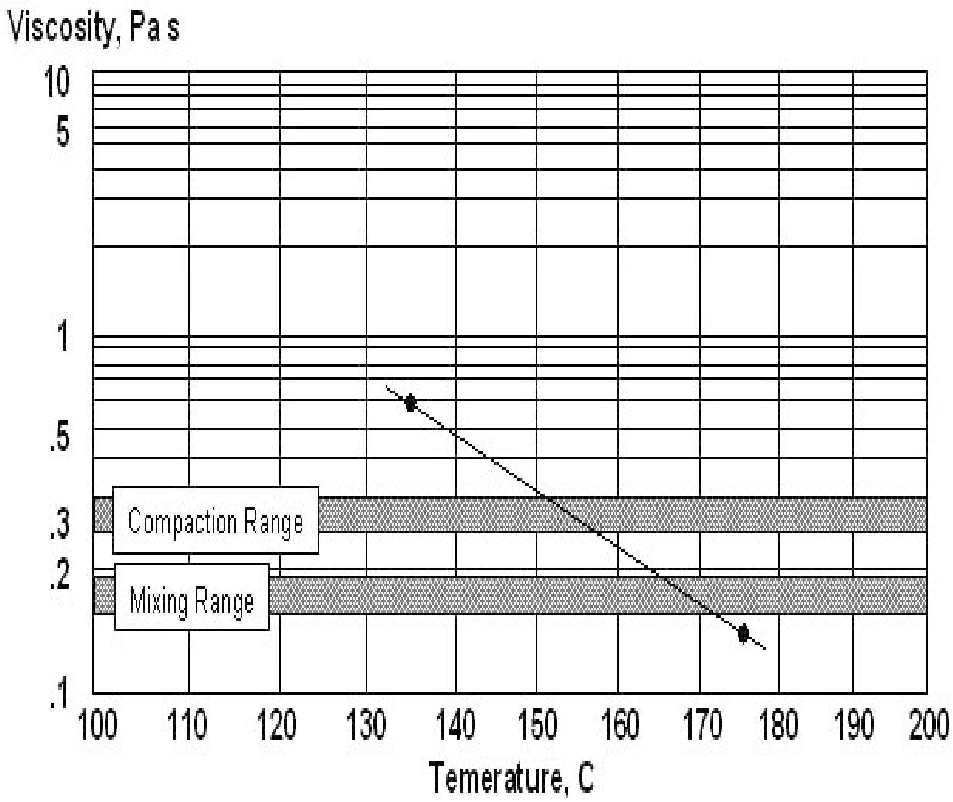

Figure 3. Typical Viscosity –Temperature Plot to Determine Compaction Temperature

$$\tau = c + \sigma \tan \o$$

Where,

τ = shear stress in the mix
c = cohesion of the mix
σ = normal stress in mix
ø =angle of internal friction

According to the De Sombre et al., shear strength for HMA is dependent on both the binder as well as the aggregate properties. The asphalt binder provides the cohesive component in HMA and the friction is provided by the aggregate particles. At a given temperature and normal stress, the cohesion of the mix depends on the amount of the binder, nature or degree of modification of the binder, and the filler used. As the amount of binder increases it becomes easier to work, (i.e., compact the mix). But as the degree of modification or filler content increases the cohesion of the mix increases which makes it more difficult to compact. With regard to aggregates, the more rounded the aggregates the lower the angle of internal friction, which reduces the shear strength of the mix. In this study six different lab samples and five different field mixes were compacted in a Finnish gyratory compactor. This compactor measured the shear stress and power required to compact each sample to 4% air voids. Samples were compacted at different temperatures. The relationships between shear and temperature necessary to compact were examined. According to this study an examination of the field temperature data combined with laboratory compaction data showed that for most mixes there was a minimum shear stress, which indicated that an optimum compaction temperature range existed (Figure 4).

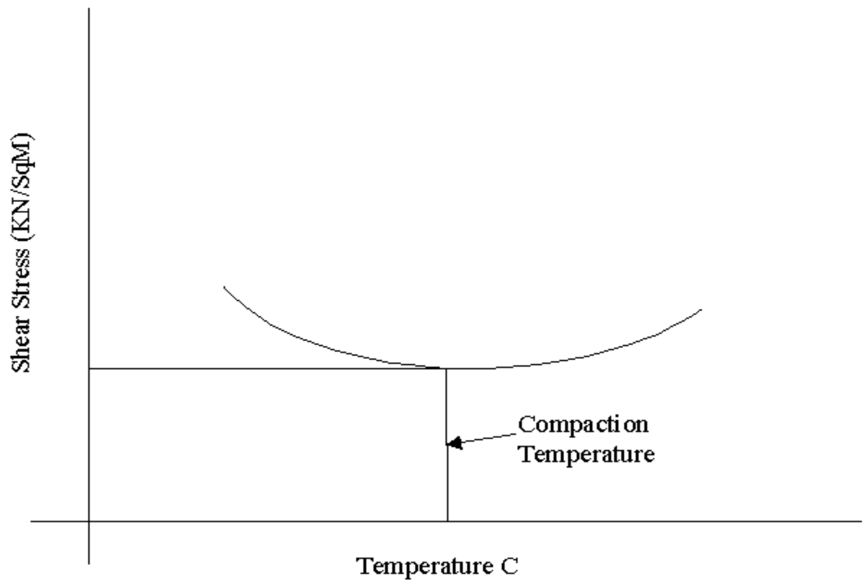

Figure 4. Relation Between Stress and Compaction Results for the Field Mixes Tested *(14)*

The following are observations from development of this background information:

- Workability of HMA depends on binder type, gradation, aggregate type, additives and temperature of the mix.
- There has been a limited attempt at quantifying the workability of HMA in the literature; however there are some limitations with this prototype.
- Instruments have been designed to measure workability based on the principle of using the torque necessary to rotate a paddle within a mix.
- The traditional method of using viscosity-temperature relationship to determine mixing and compaction temperature was developed for neat binders. It does not take into account the mix properties like aggregate properties and/or gradation shape while determining the mixing and compacting temperatures.
- There is an increasing need to determine the mixing and compacting temperatures for HMA mixes especially when modified binders are used.

RESEARCH APPROACH

To accomplish the project objectives, six separate tasks were conducted. The first task entailed development of the prototype workability device. Within the second task, mixes of expected different workability characteristics were tested with the prototype device to evaluate the limitations of the equipment and to identify needed refinements. Task 3 entailed varying several equipment characteristics to select a combination of equipment variables and to develop a tentative standard testing procedure. Next, after the equipment and test procedure were selected, samples were tested to determine the effect of material constituents on workability. Task 5 entailed a limited study to evaluate the potential of using workability results to determine compaction temperature of HMA mixes. The final task entailed preparing a final report documenting the conduct of this study. Figure 5 illustrates the overall research approach.

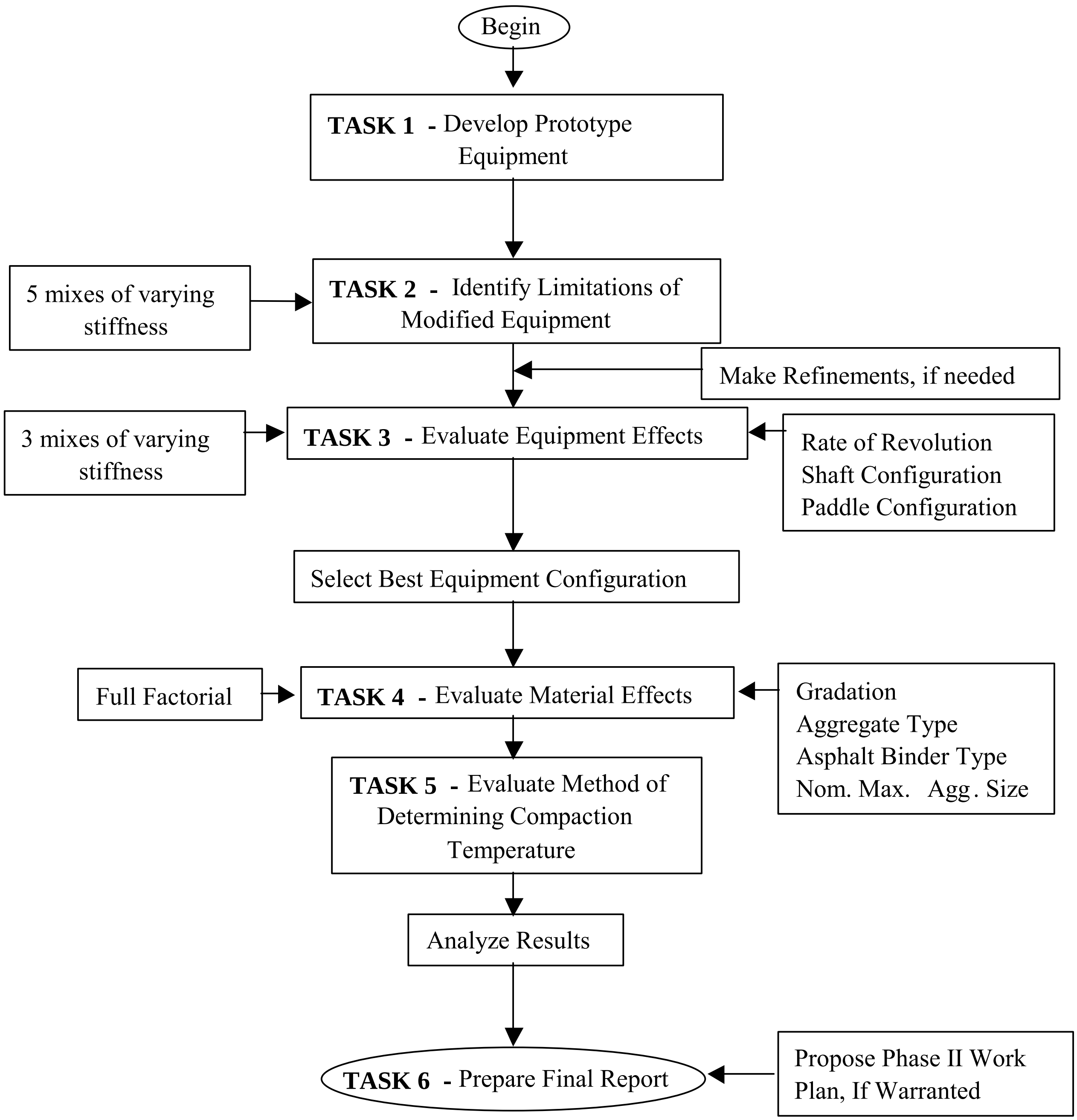

Figure 5. Overall Research Approach

Task 1 – Development of the Prototype Device

The first step in the development of a workability device was to design the prototype. NCAT had conversations with a number of manufactures about developing a prototype workability device. In the spring of 1998, Instrotek, Inc. developed the initial concept for a workability device. The initial concept utilized a Hobart mixer and an amp meter. Mix was placed within the Hobart mixing bowl and a dough hook was used to push the HMA within the bowl. The amperage required to keep the dough hook traveling at a constant speed, while pushing the mix within the bowl, was measured. This amperage was then converted to torque. An infrared temperature gun was also used to monitor temperature during the test. Even though this section is the Research Approach, the limited data obtained in this task is provided. This was done to provide the reader the background in selecting the device used to carry out the study objectives.

To evaluate this initial workability concept (Hobart mixer), four mixes were tested. The four mixes included two gradations (coarse- and fine-graded Superpave) and two binders (PG64-22 and PG76-22). These four mixes were selected because it was anticipated that each would have different workability characteristics. Results of workability testing on these four mixes are shown in Figure 6.

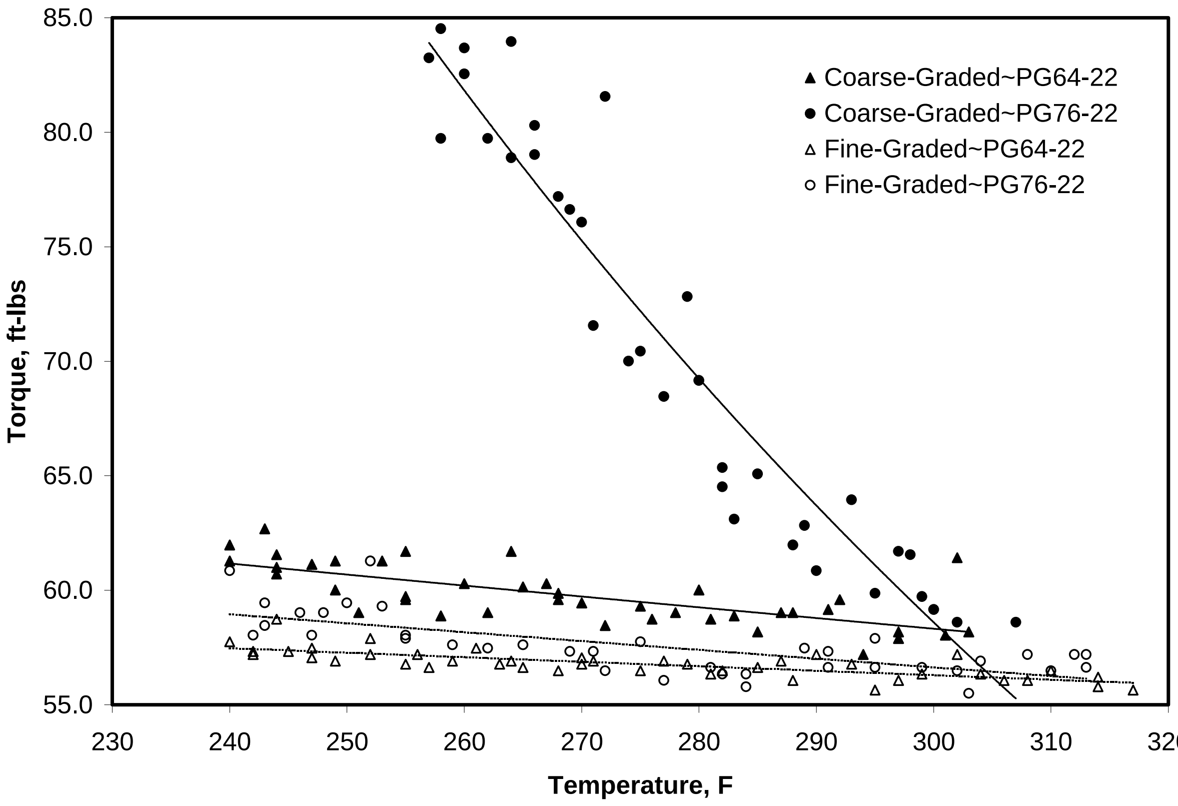

Figure 6. Results of Testing With Initial Workability Concept

Figure 6 shows that there were differences in the workability characteristics for the four mixes. This figure shows that for both gradations the mix with the PG76-22 binder was stiffer (higher torque value at a given temperature) than the companion mix with the unmodified PG64-22. Also, both of the coarse-graded mixes were stiffer than the fine-graded mixes, at a given temperature. Based on the figure, it appeared that the initial concept of measuring workability was possible. However, the equipment and procedure needed refinement before a prototype workability device could be developed.

Task 1 was designed to develop a refined, yet still prototype, piece of equipment. Based on the concept testing, the areas needing refinement included: a single vertical plane of movement, rate of revolution, paddles to replace the dough hook, sample container, and automatic torque and temperature measurements. Instrotek, Inc. took these ideas and developed the prototype equipment, which is shown in Figure 7.

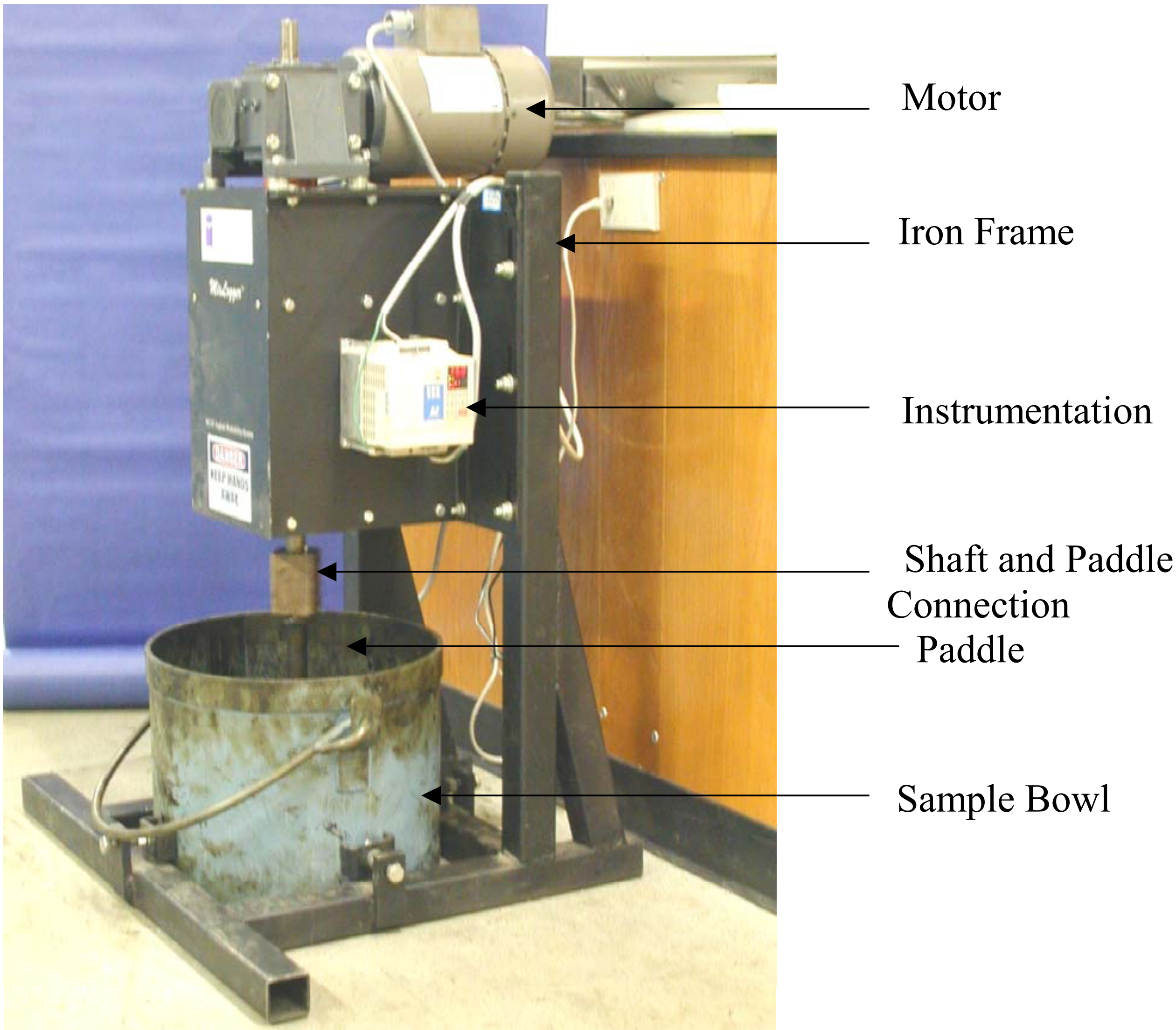

Figure 7. Prototype Workability Device

Task 2 – Identify limitations of Prototype Workability Device

Initial work with the prototype device entailed identifying the operating limits of the equipment. This was accomplished by testing five mixtures of expected varying degrees of workability. Mixes tested included:

1. Stone matrix asphalt utilizing high filler content, fibers, polymer modified PG76-22, and a very angular aggregate (granite).
2. A mixture with a gradation passing near the lower Superpave gradation control points using the PG76-22 and granite aggregate.
3. Same mixture as Item 2 except with a PG64-22 and less angular aggregate (limestone).
4. A mixture with a gradation passing near the upper Superpave control points using a PG 64-22 and crushed gravel.
5. A mixture similar to Item 4 except using rounded gravel.

Table 2 presents the mixes used during Task 2. Workability tests were conducted over a temperature range of approximately 340 to 250°F. Mixes were heated to the maximum temperature initially and allowed to cool during the test. Upon completion of testing, the data was analyzed to determine any equipment limitations (e.g., mix stiffness, whether high or low, that the device could not operate). At the conclusion, any refinements needed to the prototype device were made.

Table 2. Mixes Tested in Task 2

Aggregate Type	Gradation[1]	Nominal maximum Aggregate Size, mm	Binder Type	Replicates
Granite	SMA	19.0	PG 76-22	2
Granite	BRZ	19.0	PG 76-22	2
Limestone	BRZ	19.0	PG 64-22	2
Crushed gravel	ARZ	19.0	PG 64-22	2
Rounded gravel	ARZ	19.0	PG 64-22	2

[1] – SMA – stone matrix asphalt; BRZ – Superpave with gradation passing below the restricted zone; ARZ – Superpave with gradation passing above restricted zone.

Task 3 – Effect of Equipment Variables on Workability

This task was designed to evaluate the effect of equipment configurations on test results. Results of this testing were used in an effort to identify the best equipment configuration for measuring the workability of mixes.

Two different equipment factors were involved in this task: paddle configuration and rate of paddle revolution. These two factors should have a major impact on the ability of the device to measure workability. The paddle configuration should be such that it continuously remixes the sample and does not create a shear plane through the mixture. A shear plane created within the sample would show a consistent workability (torque) over a given temperature range because of a lack of resistance. If the rate of revolution for the paddle is too fast, a shear plane can also be created.

Testing for this task included three of the mixes used in Task 2. The three mixes included the stiffest, least stiff, and one between the extremes based on the Task 2 testing.

A full factorial experiment was conducted using two levels of paddle configuration and two levels of rate of revolution. Instrotec, Inc. manufactured the paddles after discussions with NCAT. The two rates of revolution included within the experiment were 5 and 15 rpm. At the conclusion of testing, the data was analyzed to determine which set of equipment variables would provide the most suitable workability values over the temperature interval evaluated.

Task 4 – Evaluation of Material Effects

Within this task, the effect of material properties was evaluated. Included in the test matrix were aggregate type (and, thus, physical properties), binder type, gradation shape, and nominal maximum aggregate size (NMAS). Table 3 shows the test matrix for this task.

Table 3. Test Matrix for Task 4

		12.5 mm		19 mm	
		ARZ	BRZ	ARZ	BRZ
Granite	64-22	2	2	2	2
	70-22	2	2	2	2
	76-22	2	2	2	2
Crushed Gravel	64-22	2	2	2	2
	70-22	2	2	2	2
	70-22	2	2	2	2
Limestone	64-22	2	2	2	2
	70-22	2	2	2	2
	76-22	2	2	2	2

Mix designs were conducted only for those combinations containing the PG 64-22 binder. The combinations containing the PG 70-22 and PG 76-22 binders utilized the optimum binder content determined for the corresponding PG 64-22 combination. Two replicates of each mix were tested in the workability device. Data was collected over a temperature range of approximately 170 to 120°C. At the conclusion of testing, the data was analyzed to evaluate the effect of the four main factors on workability.

Task 5 – Evaluate Method of Determining Compaction Temperature of HMA

After completion of testing in Task 4, the data was evaluated in an effort to investigate a method of determining the compaction temperature of HMA mixes. To try and verify the compaction temperatures obtained by the method hypothesized, a limited compaction study was conducted. For this study a Superpave gyratory compactor (SGC) was used as a measure of compactibility. The compactor was a Pine Instrument Company gyratory compactor model AFG1A. This SGC has an added feature not common to most models to measure the gyratory shear developed inside the mix as it is compacted. The compactor that was used had the capability to calculate a value called gyratory shear ratio at each gyration. A schematic diagram of the different forces that act on the sample as it gets compacted can be seen in Figure 8.

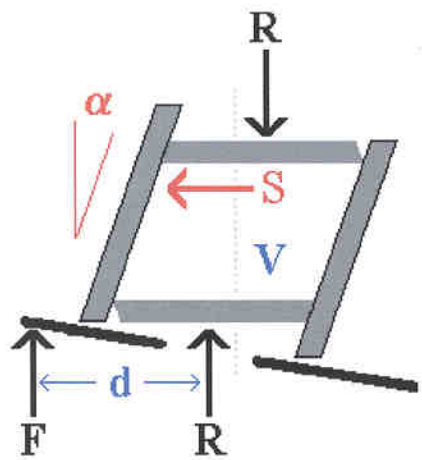

Figure 8. Simple Shear Diagram

The different letters that represent the various forces and dimensions in the figure are as follows:

R = The ram force, lb
F = Force required to tilt the mold by an angle of 1.25 degrees, lb
d = Lever arm distance where the force is applied to tilt the mold, in
α = The angle of gyration
V = Volume of the mix, in^3
S = Gyratory shear, psi
A= Area of the sample in^2
P = R / A = Pressure on the sample, psi

The force that was required to maintain the angle of gyration is a function of the lever arm distance (d) , mix stiffness and the ram pressure (P). This force was measured by the compactor and the gyratory shear was then computed as:

$$S = (F*d) / (V) \qquad \text{Eq. 2}$$

Assuming that gyratory shear was a function of ram pressure the gyratory shear was normalized with ram pressure as:

$$\sigma = S / P \qquad \text{Eq. 3}$$

Where,

σ is the gyratory shear ratio.

This experiment was conducted on nine of the 36 mixes shown in Table 3. All three asphalt binders were included with the 12.5 mm NMAS-BRZ gradation-limestone aggregate, 12.5 mm

NMAS-ARZ gradation-limestone aggregate, and 19.0 mm NMAS-BRZ gradation-granite aggregate combinations.

Task 6 – Prepare Final Report

At the conclusion of all testing, a report was written that documents all test results and analysis of the test results.

MATERIAL PROPERTIES

Aggregates

Four different types of aggregate were used in this study: granite, limestone, crushed gravel and rounded gravel. The physical properties of the aggregates are reported in Table 4.

Gradations

Five different gradations were used in this study. There were two gradations for the two nominal maximum aggregate sizes, one finer (above the restricted zone (ARZ)) and one coarser (below the restricted zone (BRZ)). The gradations used in this study are shown in Table 5. Except for the fraction passing the 0.075 mm sieve, a single aggregate type was used. Marble dust was used as the filler (passing 0.075 mm sieve) fraction in all the mixes. Except for the SMA, the overall aggregate gradation consisted of about 96 percent aggregate and 4 percent marble dust. For the SMA the amount of filler was 9 percent. In addition, cellulose fiber was added at 0.3 percent by weight of the total mix mass for the SMA. For gradations containing the rounded gravel, aggregate sizes below No. 4 (4.75mm) were not available so crushed gravel was used instead of rounded gravel.

Binder Properties

Three different binders were used in the study: PG 64-22, PG 70-22 and PG 76-22. The PG 64-22 was an unmodified binder while the PG 70-22 and PG 76-22 were polymer-modified binders with varying concentration levels of styrene butadiene styrene (SBS) polymer. The original and RTFO aged properties of all three binders are shown in Table 6. Based upon the failure temperatures shown in Table 6, the PG 64-22 binder met Superpave performance grading high temperature requirements up to 66°C. The PG 70-22 met requirements to 71°C and the PG 76-22 met high temperature requirements to 77°C**.**

Workability in this study was evaluated between temperatures of approximately 120° C and 180° C. To understand the behavior of binder viscosity in this temperature range, viscosities for the three binders were determined by a rotational viscometer over this temperature range. The rate of revolution of the spindle in the rotational viscometer was 20 RPM during these viscosity measurements.

Table 4. Aggregate Properties

Property		Test Method	Aggregate Type			
			Granite	Limestone	Crushed Gravel	Rounded Gravel
Coarse Aggregates						
Bulk Specific Gravity		AASHTO T-85	2.649	2.713	2.581	2.610
Apparent Specific Gravity		AASHTO T-85	2.708	2.744	2.639	2.645
Absorption (%)		AASHTO T-85	0.817	0.415	0.851	0.513
Flat and Elongated (%) 3:1, 5:1	19.0 mm	ASTM D4791	14, 0	10, 0	4, 0	0, 0
	12.5 mm		16, 0	6, 0	16, 2	6, 0
	9.5 mm		9, 1	16, 3	19, 2	14, 1
Los Angeles Abrasion (%)		AASHTO T-96	33	26	30	46
Percent Crushed (%) (2F)			100	100	80	0
Fine Aggregates						
Bulk Specific Gravity		AASHTO T-84	2.656	2.640	2.618	2.618
Apparent Specific Gravity		AASHTO T-84	2.710	2.731	2.640	2.640
Absorption (%)		AASHTO T-84	0.75	1.27	0.32	0.32
Fine Aggregate Angularity (%)		AASHTO T-33 (Method A)	45.9	42.9	48.2	48.2
Sand Equivalency (%)		AASHTO T-176	92	93	94	94
*Since aggregates below No. 4 were the same for both rounded and crushed gravel the properties are reported the same						

Table 5. Gradations for All the Mixes

Sieve Size		12.5 mm		19.0 mm		SMA
Inches	mm	ARZ	BRZ	ARZ	BRZ	
1	25.0	-	-	100	100	100
¾	19.0	100	100	95	95	100
½	12.5	95	95	80	80	95
3/8	9.5	86	86	68	68	26
No. 4	4.75	61	61	45	45	20
No. 8	2.36	45	33	41	29	16
No. 16	1.18	35	23	31	19	14
No. 30	0.6	26	16	24	14	13
No. 50	0.3	19	13	19	11	12
No. 100	0.15	11	9	11	9	10
No. 200	0.075	4	4	4	4	9

Table 6. Binder Properties

Original Binder						
Properties	PG 64-22		PG 70-22		PG 76-22	
Test Temperature °C	67.1	73.0	70.0	76.0	76	82.0
G^* (Pa)	1211	577.1	1420	746.1	1383	812.9
δ(degrees)	87.75	88.58	78.27	79.57	66.83	67.33
$G^*/\sin\delta$ (kpa)	1.212	0.5773	1.450	0.7587	1.505	0.881
Failure Temperature, °C	68.6		73.4		82.0	
Rolling Thin Film Oven Aged						
	PG 64-22		PG 70-22		PG 76-22	
Test Temperature, °C	61.0	67.0	69.9	76.6	76	81.9
G^* (Pa)	4259	1877	2378	1249	2210	1342
δ(degrees)	84.51	86.13	75.05	76.57	62.93	63.12
$G^*/\sin\delta$	4.278	1.882	2.462	1.284	2.482	1.504
Failure Temperature, °C	65.9		71.0		77.4	

Typically the relation between viscosity and temperature is plotted on a semi-log scale with viscosity on the log scale, but in this figure viscosity was plotted on a linear scale. The reason for doing this was if viscosity had been plotted on the log scale the relationship will appear linear and the relative effect of temperature on viscosity cannot be distinguished. Figure 9 shows that as the temperature increased from 120°C to 180°C the viscosity of all three binders decreased. However the rate of decrease was not constant. Initially, there was a large reduction in viscosity. However, after reaching a temperature of about 145°C the rate of decrease in viscosity was much lower. Even though the magnitude of viscosity at any particular temperature for all three binders was different, the general trend of all the curves was the same.

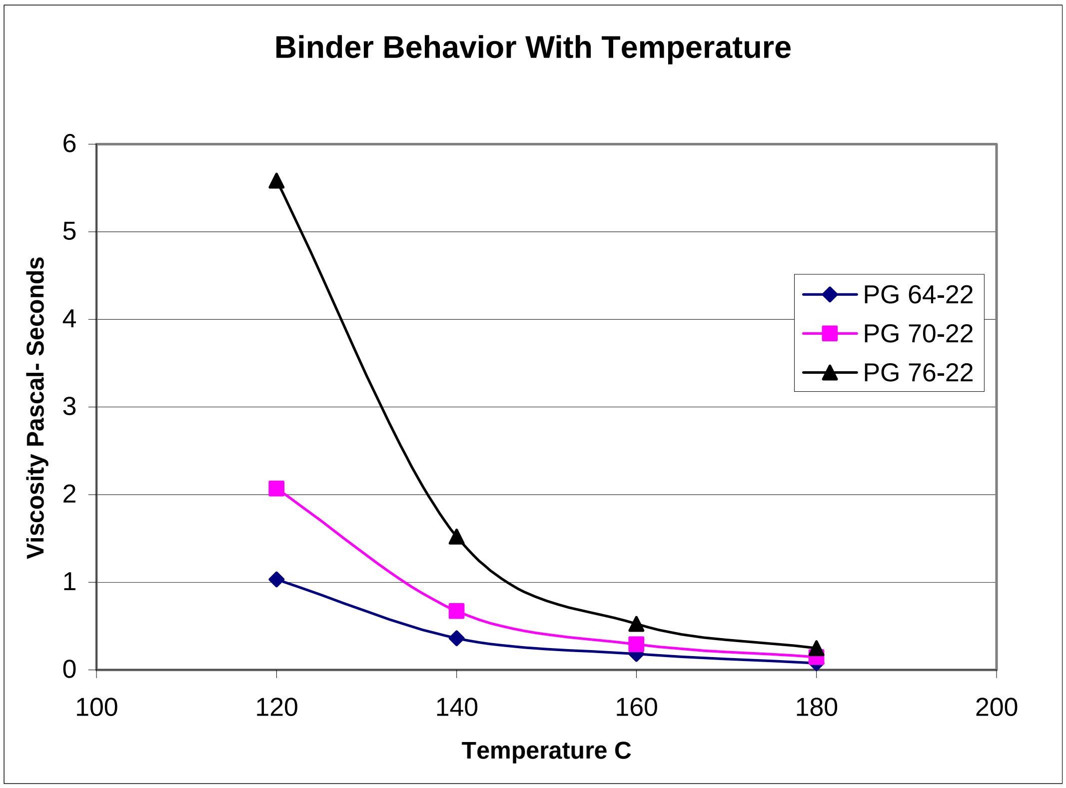

Figure 9. Viscosity Temperature Plots

During the developmental stage of the workability device, mixes were tested with different rates of revolution of the paddle (Task 3). This was done to determine the rate of revolution that best differentiates the workability of mixes. The different rates of revolution also imply that the mix was being worked at various shear rates. Since each binder may have a shear rate dependency, this binder property was also evaluated. The effect of shear rate on binder viscosity within the temperature range of 120 to 180°C is presented in Figures 10, 11 and 12. For this testing, the shear rates within the Brookfield rotational viscometer were 10, 20, 30, and 50 RPMs. These figures show that there was very little effect of rotational speeds on the viscosity of the binders. There did appear to be a small effect for both of the modified binders at 120°C but since the workability test was generally stopped at 120°C, this was not considered significant to the results of the study. This suggests that measurement of workability for a given gradation and binder should not be influenced by any non-Newtonian behavior of the binder for the temperature range used in this study.

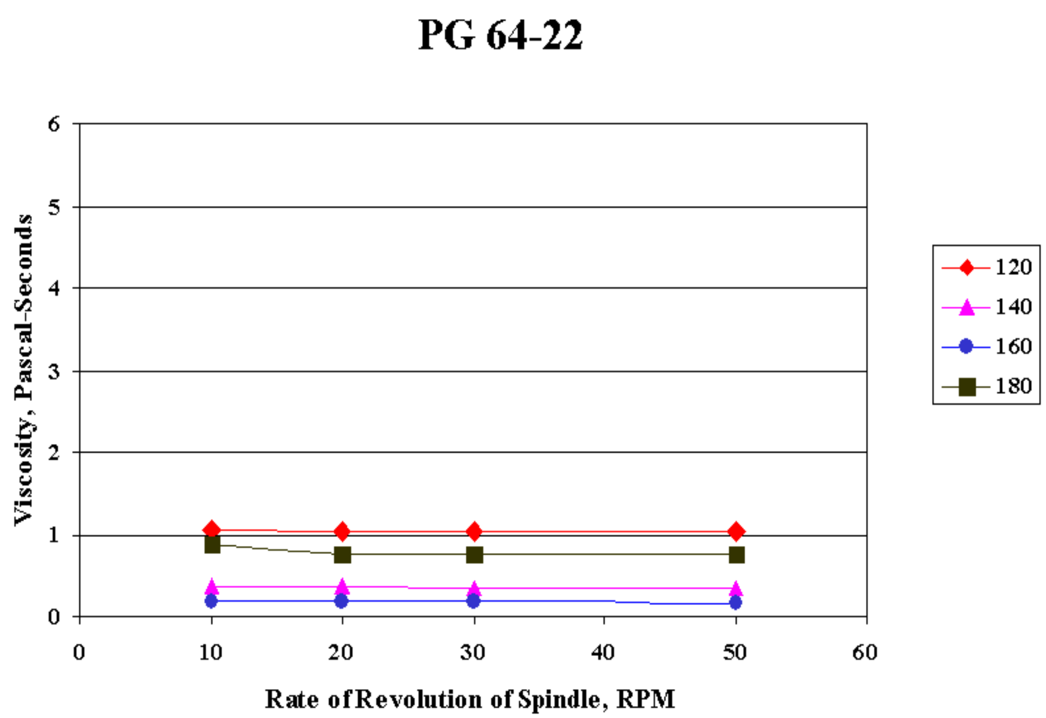

Figure 10. Effect of Shear Rate on PG 64-22

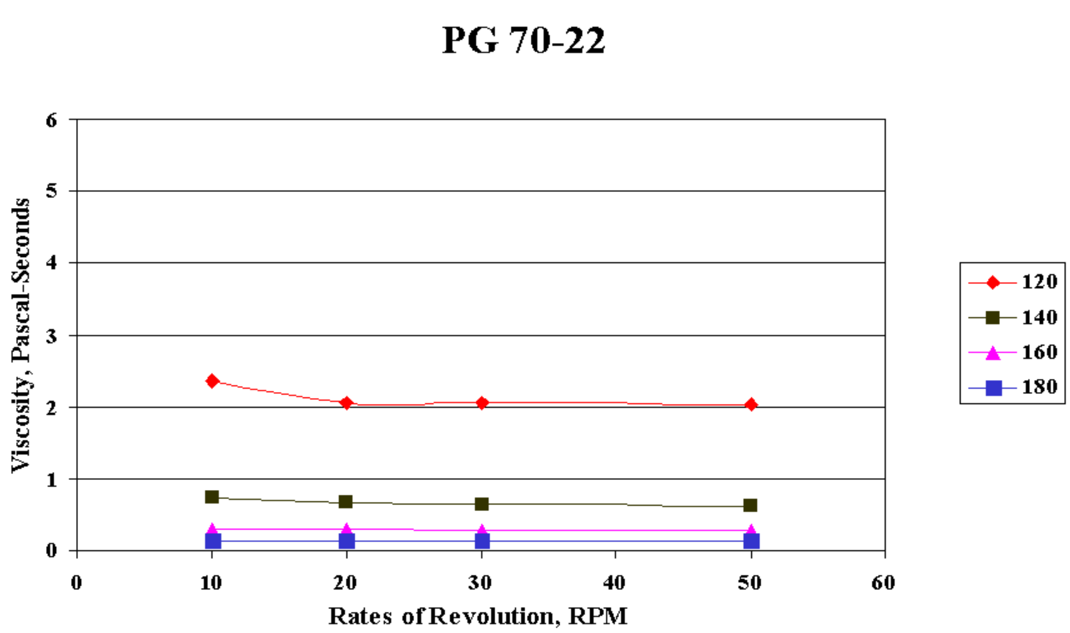

Figure 11. Effect of Shear Rate on PG 70-22

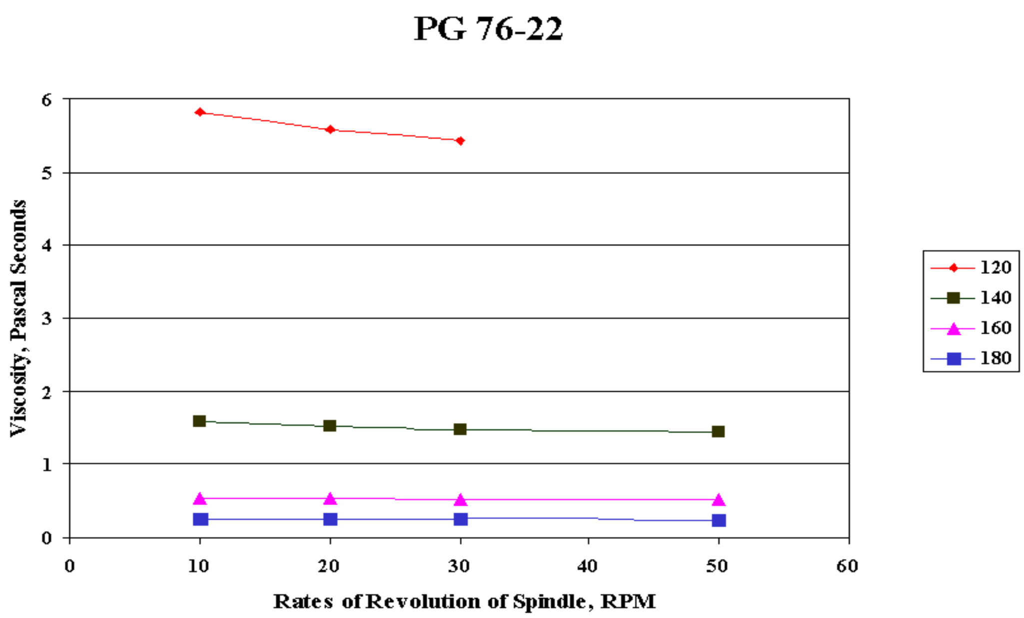

Figure 12. Effect of Shear Rate on PG 76-22

Viscosity values obtained with the rotational viscometer at 120°C and 180°C at 20 RPM were plotted on a semi-log scale and joined by a straight line for each of the binders. Temperature values corresponding to a viscosity of 0.28 Pascal seconds were utilized as the compaction temperature. Figures 13, 14, and 15 present this data. The compaction temperatures obtained using this traditional approach for the three binders were 149°C, 164°C and 179°C for the PG 64-22, PG 70-22 and PG 76-22, respectively.

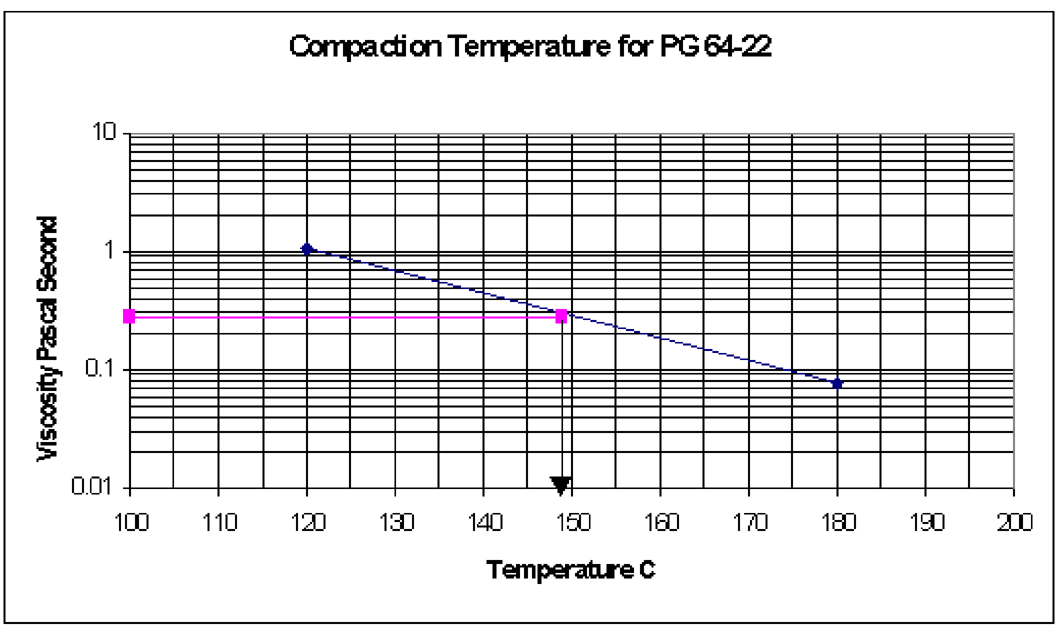

Figure 13. Compaction Temperature for PG 64-22

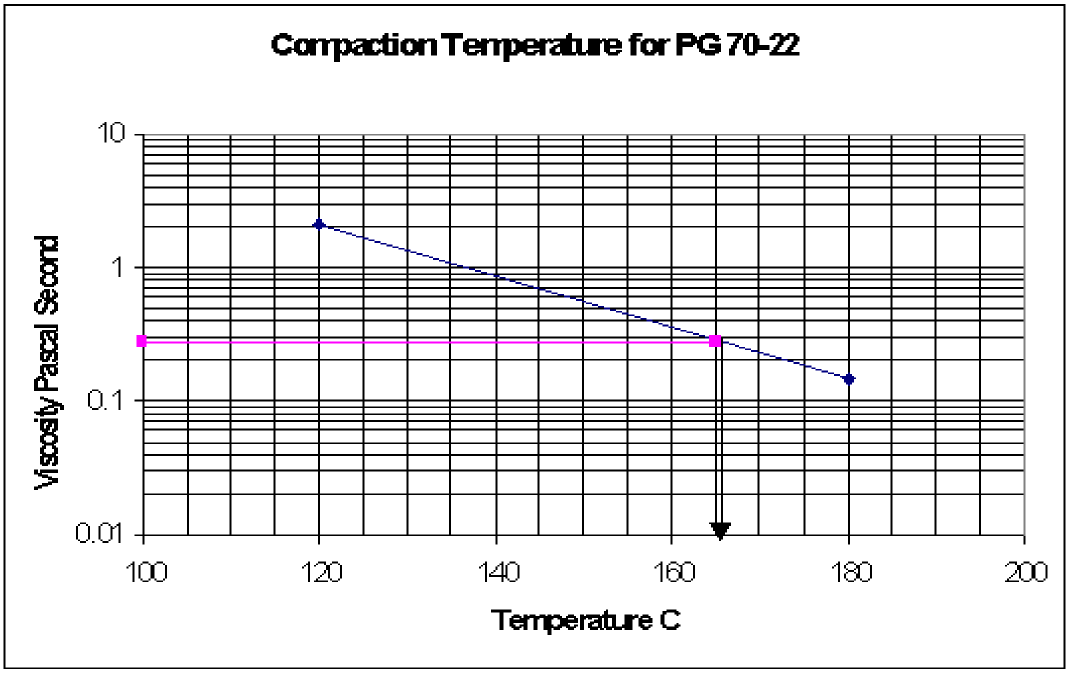

Figure 14. Compaction Temperature for PG 70-22

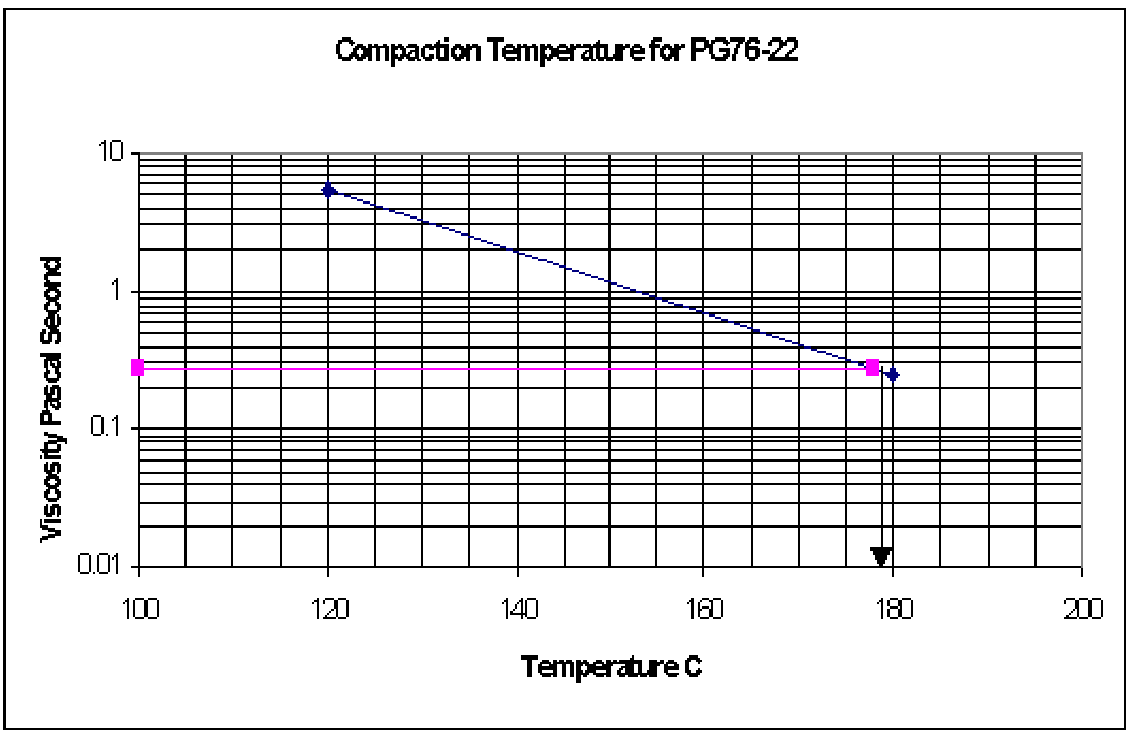

Figure 15. Compaction Temperature for PG 76-22

Mix Designs

Mixes were designed according to the Superpave mix design methodology. The optimum binder contents for all of the mixes are presented in the Table 7. All the mix designs were initially carried out using the PG 64-22 binder. Mixes containing the two modified binders were combined at the same binder content determined for companion PG 64-22 mixes. For the SMA, optimum binder content used was 6.3 percent of the total mix mass and a PG 76-22 was used as the binder.

Table 7. Optimum Binder Content of the Mixes

		Optimum Binder Contents (%)			
		12.5 mm NMAS		19.0 mm NMAS	
Aggregate	Binder	ARZ	BRZ	ARZ	BRZ
Granite	PG 64-22 PG 70-22 PG 76-22	5.2	5.1	4.3	4.2
Limestone	PG 64-22 PG 70-22 PG 76-22	4.2	4.9	4.2	4.7
Crushed Gravel	PG 64-22 PG 70-22 PG 76-22	4.7	4.5	4.0	4.2
Rounded Gravel	PG 64-22	4.2	---	---	---

TEST RESULTS AND ANALYSIS

Within this section, test results and the analyses conducted to accomplish the project objectives are presented. Within the Research Approach section, the development of the workability device was discussed as Task 1. Therefore, results within this section are provided for Tasks 2 through 5.

Data Reduction

Prior to discussing test results, it is necessary to describe the type of data generated. The raw data generated include torque and temperature measurements. The units in which they were measured were inch-pound and degrees Celsius, respectively. A typical plot of the torque and temperature for a given mix is illustrated in the Figure 16. From the figure it can be seen that there is an initial noise in the data. The paddle rotating in the sample container before the mix is introduced causes much of this noise seen near the 70°C temperature. Aggregate batch sizes needed to perform the workability test were 20,000 grams. Therefore, the mixture had to be distributed into two containers for short-term aging. The noise in the data at temperatures between 160 and 170°C and torque values below 300 in-lb represent addition of the first container of mix prior to the introduction of the second container.

In Figure 17, the general trend of all the points (for a different sample) can be seen without the initial noise. On this figure a trend line was also included. At high temperatures, torque values were at their lowest (near 200 in-lb) and relatively constant. As the temperature decreased, torque values increased. These trends were observed for all of the different mixes tested in this study. Another observation about Figure 17 was that there were data points that appeared to have torque values much higher than the data trend. The probable reason for these high values was aggregates getting caught between the paddle and sample container causing large torque values. To identify potential outliers, regression equations for each test were determined.

The method selected for identifying potential outlying data was to develop regressions between torque and temperature and evaluate standardized residuals. The model selected for developing the regressions was an exponential model. An exponential model has the following form:

$$y = \alpha e^{\beta x} \qquad \text{Eq. 4}$$

Where,

y = response (torque);
α, β = regression statistics; and
x = independent variable (temperature)

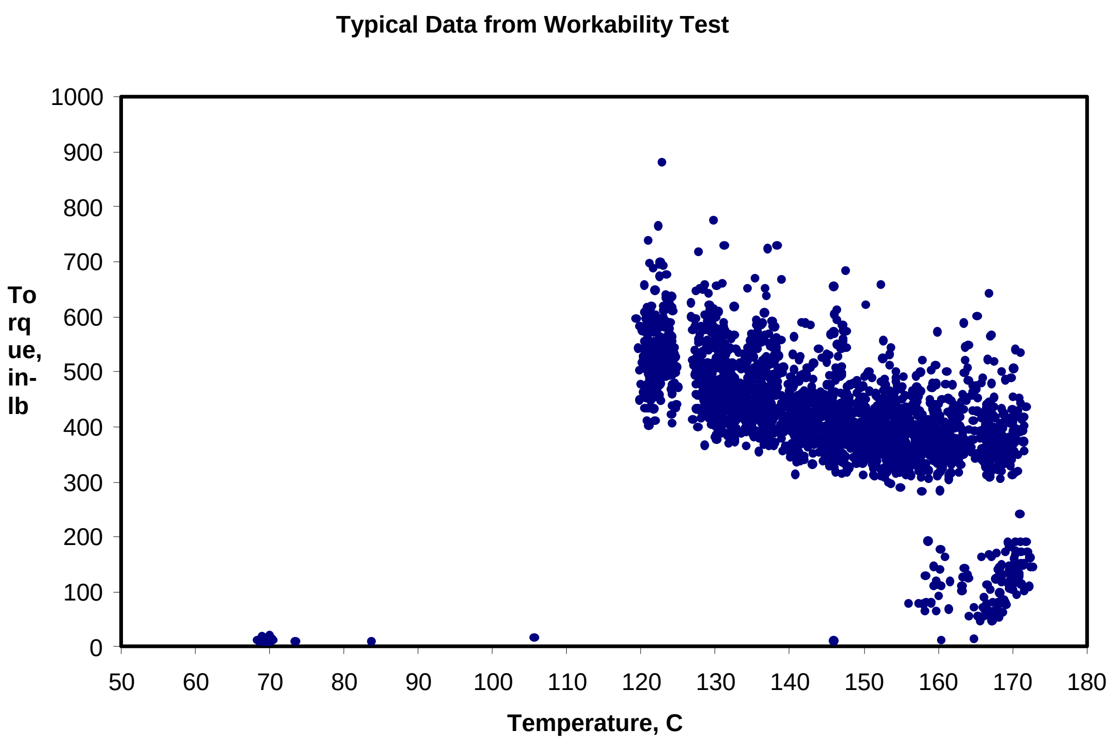

Figure 16. Sample Raw Data with Noise Generated by the Workability Device

The steps in identifying outliers were first to regress the dependent data (ln[torque]) to the independent data (temperature). Regressions were conducted for each of the mixes tested. Based upon the regression statistics for a given mix, the residuals for each observation were calculated. For a given mix, there were between 2500 and 3500 observations, depending upon the length of the test. A residual is the difference between a given observation and its predicted value from the regression. Standardized residuals were then calculated as follows:

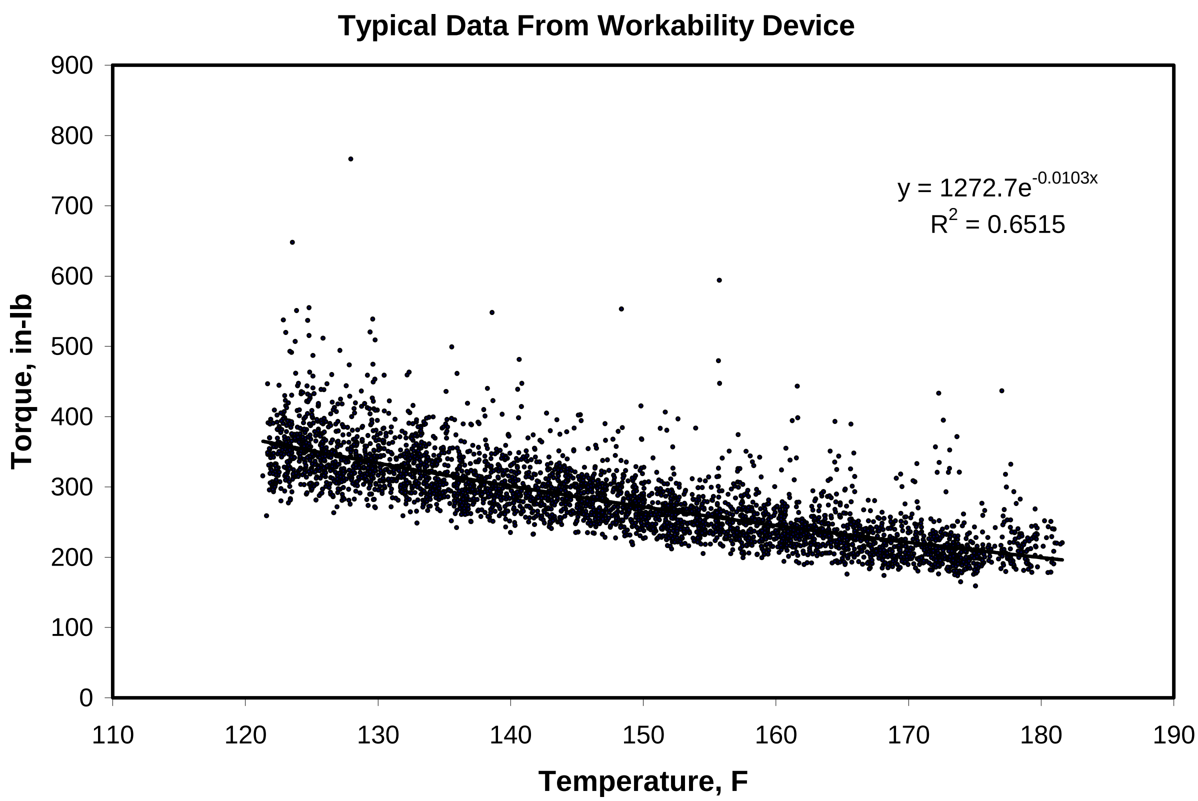

Figure 17. Typical Data Without Initial Noise

$$d_{ij} = \frac{e_{ij}}{\sqrt{\frac{(n-1)}{n} MS_E}} \qquad \text{Eq. 5}$$

Where,

d_{ij} = standardized residual for an observation;

e_{ij} = residual (observation minus predicted value) for an observation;
n = number of observations; and
MS_E = variance of residuals.

Montgomery *(13)* has indicated that for a normal population, standardized residuals should be approximately normal with a mean of zero and a variance of one. Because of the extremely large sample size obtained for torque, the data was assumed normal. A standardized residual for a regression is an indication of how far a given data point resides from the best-fit line.

Approximately 68 percent of the data points should be within ±1 standardized residuals, 95 percent should be within ±2, and 99.9 percent should be within ±3 standardized residuals. Montgomery suggests that test results with standardized residuals greater than 3 or 4 are potential outliers. For the purposes of this study, observations with a standardized residual greater than 3 were considered outliers.

Figure 18 shows the same data as Figure17 with the outliers removed. With the outlying data removed, a new regression was conducted.

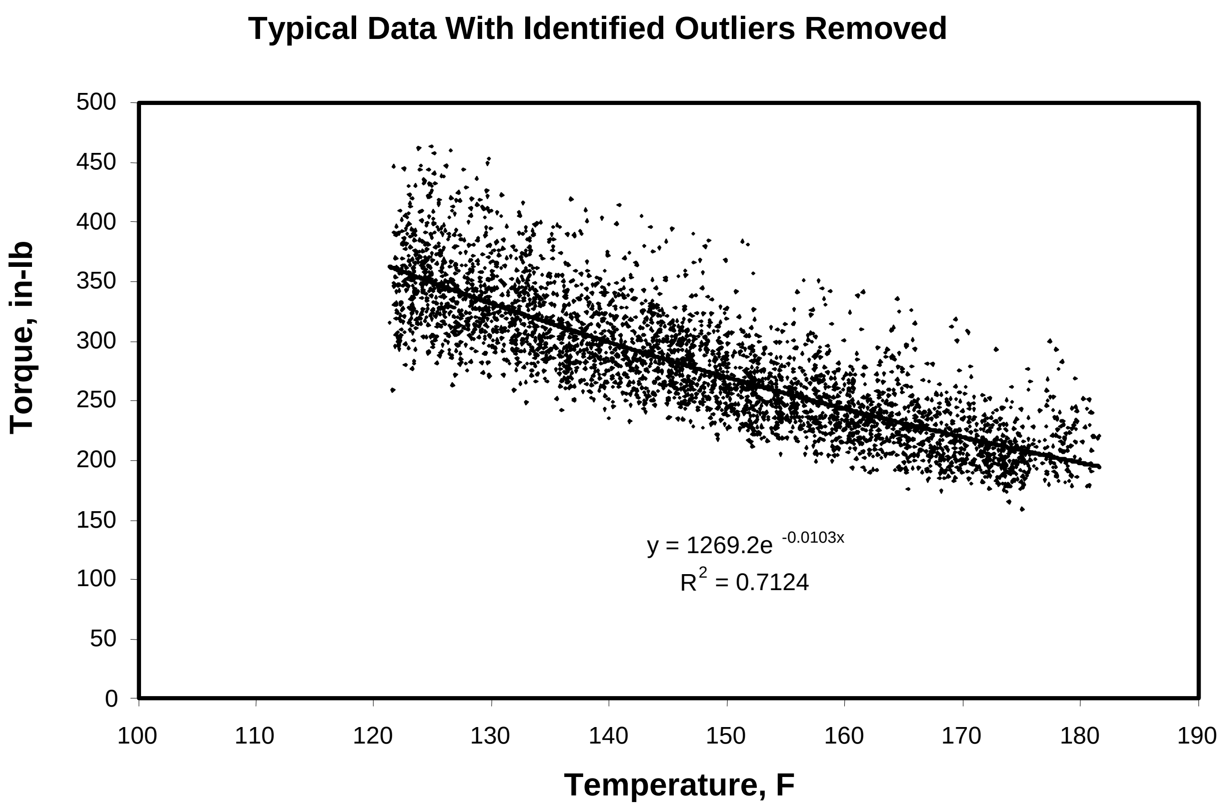

Figure 18. Typical Test With Outliers Removed

Task 2 - Identify Limitations of Prototype Workability Device

A paddle was designed in such a way that problems identified with the initial paddle (dough hook) were minimized. The paddle used in this section was identified as Paddle A and is shown in Figure 19. Paddle A had three blades. The blades of the paddle were kept at different elevations so that the chance of developing a shear plane during the test was minimized. The angle of the bottom blade was kept at 45 degrees to the direction of rotation to lift mix from the bottom of the container. The middle blade was kept perpendicular to the direction of rotation of the paddle, but it was curved slightly to the inside. This was done in an effort to prevent the segregation of larger particles toward the edge of the bowl and to continuously remix these larger particles with the remaining sample. The top blade was inclined at 45° to the direction of rotation of the paddle to force the mix downward.

Once the paddle was designed it was tested with five different types of HMA mixes, which were believed to have different stiffnesses (Figure 20). The mixes included a stone matrix asphalt, coarse-graded Superpave mix with a cubical aggregate (granite) and polymer-modified binder, coarse-graded Superpave mix with a limestone aggregate and unmodified binder, fine-graded Superpave mix with a crushed gravel aggregate and unmodified binder, and a fine-graded mix with rounded gravel. These mixes were selected because it was anticipated they would have different workability.

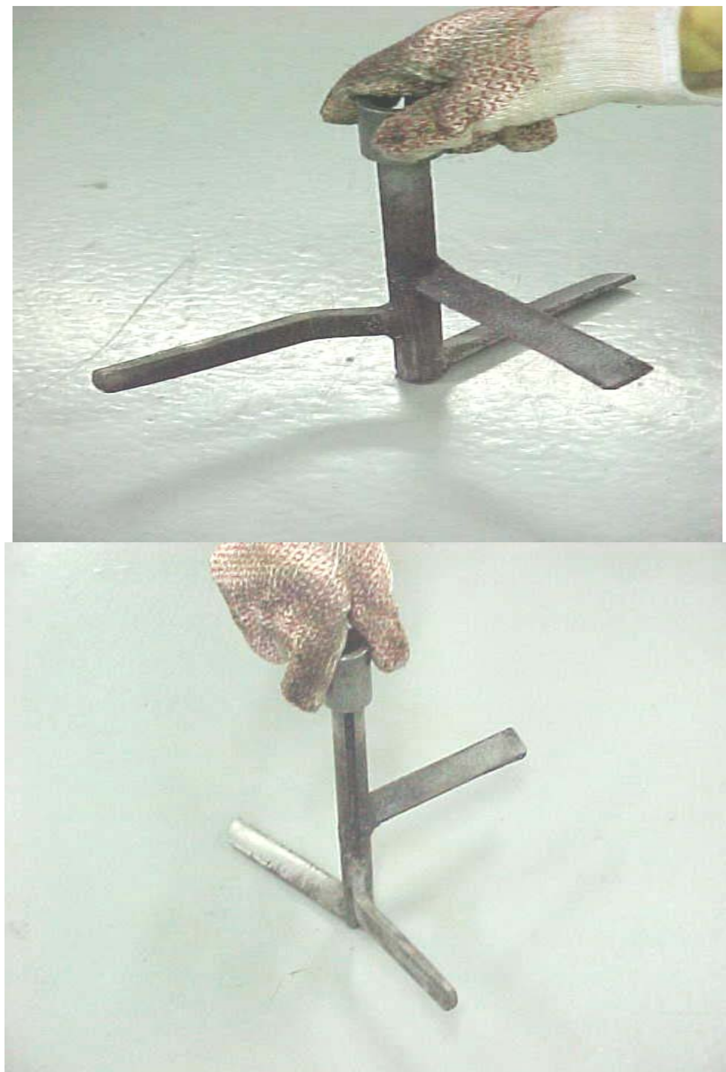

Figure 19. Two Views of Paddle A

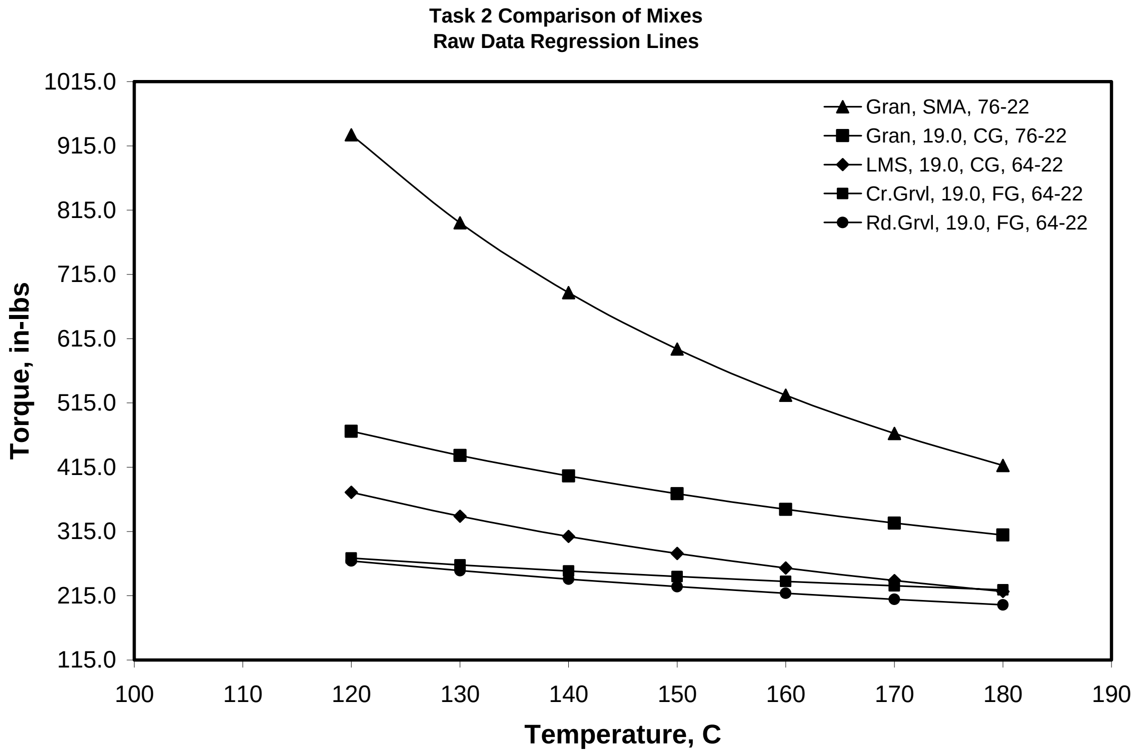

Figure 20. Comparison of Mixture Workability

As expected, there were different torque-temperature relationships for each of the five mixes, signifying the different workabilities. The SMA mixture had the highest values of torque at all temperatures. This was expected as the SMA contained an angular aggregate (granite), polymer modified PG 76-22, cellulose fiber, and high filler content. The workability curve for the mix that was on the coarse side of restricted zone, combined with a polymer modified binder and the angular granite aggregate was higher than the remaining dense-graded mixes at a given temperature. The torque values were expected to be higher due to the presence of the modified binder binder and angularity of the aggregates. Out of the remaining three mixes, the limestone mix having a gradation on the coarse side of the restricted zone had slightly higher torque values at the lower temperatures than the two fine-graded mixes, even though all were mixed with unmodified binder. Mixes that were on the fine side of the restricted zone and mixed with rounded and crushed gravel appeared to have more or less the same workability. This was contrary to expected. It was expected that there would be a difference in the workabilities due to the different aggregates shape and texture. However when the aggregates were batched, due to the non-availability of rounded gravel below the 4.75 mm sieve size, crushed fine aggregates were used in the blend. This may explain the similarity in the two fine-graded mixes.

Modifications Done After This Task:

- By the end of this stage it was observed that the length of the blades could cause a problem. In the initial design of the blades of the paddle, they were about ½ inch from the sides of the mixing bowl. For this reason larger aggregate particles occasionally wedged between the bowl and paddle, resulting in spikes in the torque measurements. To reduce this problem the length of the blades of the paddle was reduced by an inch.

Effect of Equipment Variables on Workability

This testing was conducted to select the best rate of revolution of the paddle and type of paddle configuration. In this experiment, two paddle configurations were tested. One was the Paddle A tested in Task 2; the second, Paddle B (Figure 21), was a modification of Paddle A. When Paddle A was designed the effectiveness of the top blade of the paddle was unclear. So Paddle B was developed to exclude the top blade.

Figure 21. Picture of the Paddle B Used in the Second Stage of Testing

Three rates of revolution: 5, 10 and 15 RPM`s, were selected to be evaluated. Three mixes were selected from the five mixes used in the previous series of tests. The three mixes selected were the SMA, coarse-graded limestone and fine-graded rounded gravel because they had the least, intermediate and highest workabilities in the previous section, respectively.

When the paddle was rotated a 5 RPM with the SMA, the motor tended to stop as the speed was too slow and the mix got very stiff very quickly. The reason for this was that the torque generated to rotate the SMA was greater than the capacity of the motor. Subsequent tests at 5 RPM with the remaining mixes were terminated. Results of the relationships between torque and temperature for the 10 and 15 RPMs can be seen in Figures 22, 23, and 24.

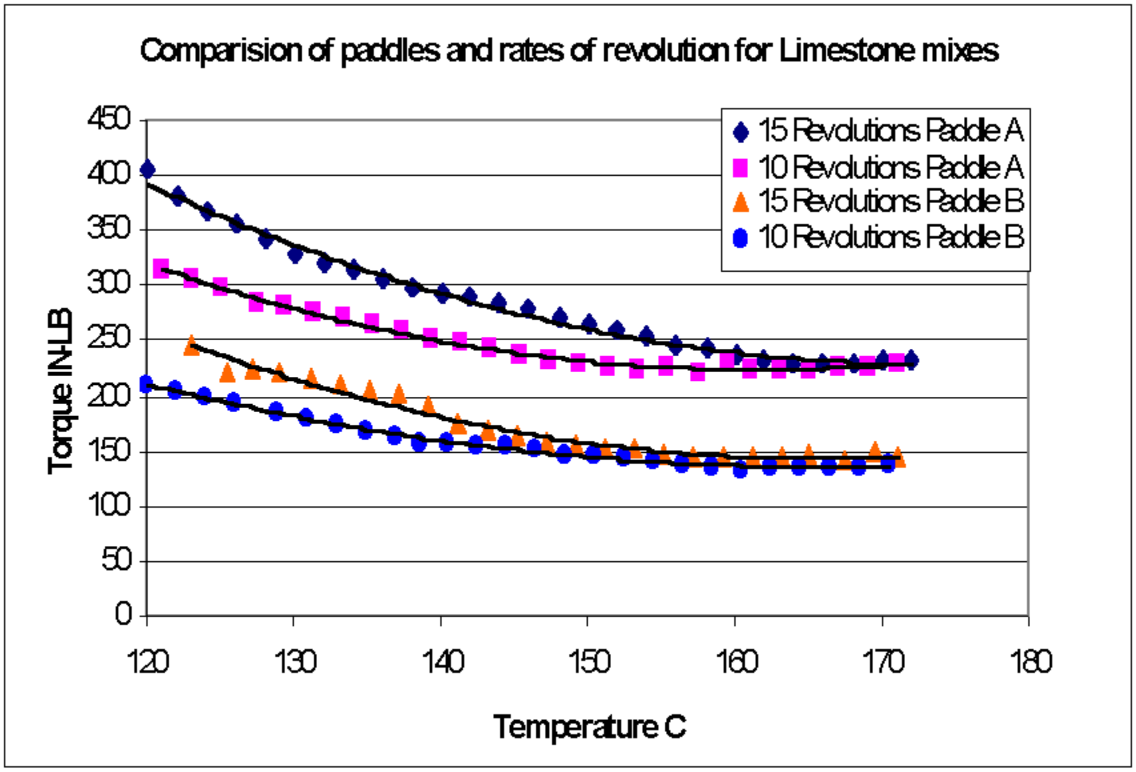

Figure 22. Comparison of Paddles and Rates of Revolution for Limestone Mixes

Limestone Mixtures

From Figure 22 it can be seen that the difference in torque due to RPM's was minimal at higher temperatures for a given paddle configuration. At lower temperatures, Paddle A generated more torque when compared to Paddle B. Even though there were differences in the workability curves for the different paddle and RPM combinations the general trend was similar in all cases. Out of all the combinations the 15-RPM Paddle A had the widest range in workability for the temperature range tested.

SMA Mixtures

Figure 23 shows the results of testing on the SMA mixture. Again, all four equipment configurations provided similar trends. Also, Paddle A rotated at 15 RPM provided the widest range in torque values for the temperatures encountered.

Rounded Aggregates

For mixes with rounded gravel (Figure 24), even though there was a difference in the magnitude of the workability curves for the different combinations of paddle type and RPM, the general trend of the curves were again similar. The figure shows that the workability of the fine-graded, rounded gravel mixes was less sensitive to temperature when compared to the stiffer mixes. The general trend of all the combinations was the same. The 15-RPM Paddle A had the widest range of torque values for the temperature range tested.

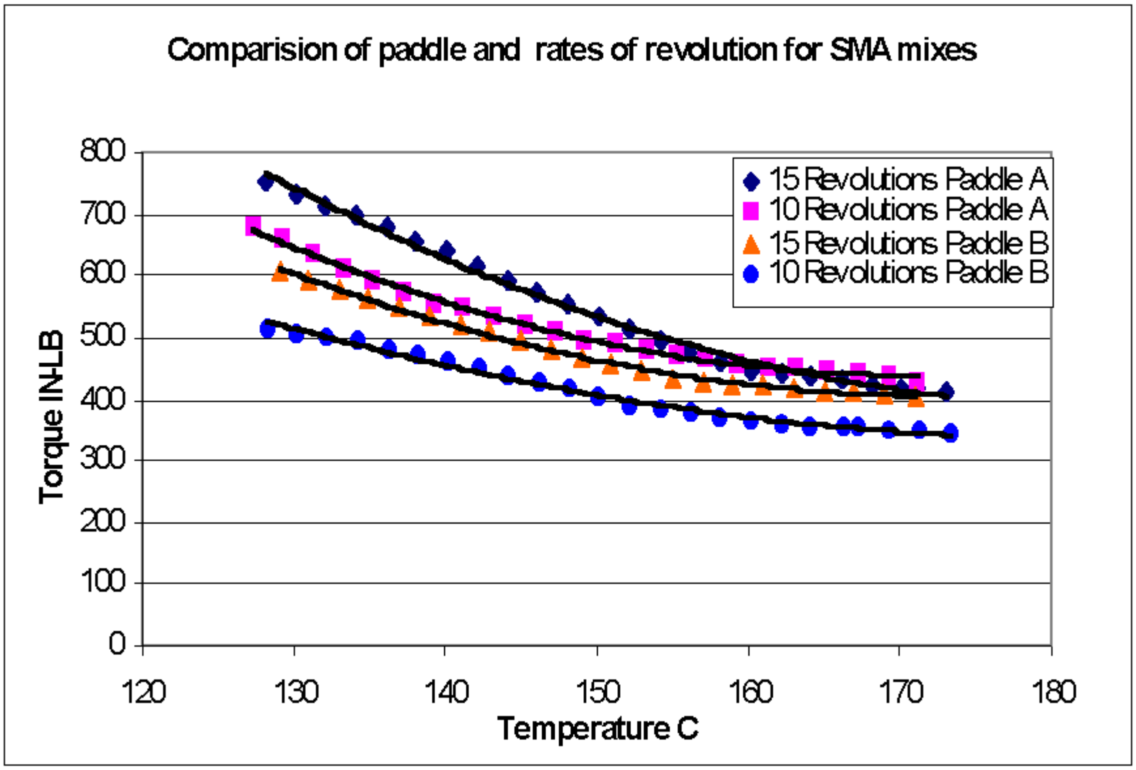

Figure 23. Comparison of Paddles and Rates of Revolution for SMA Mixes

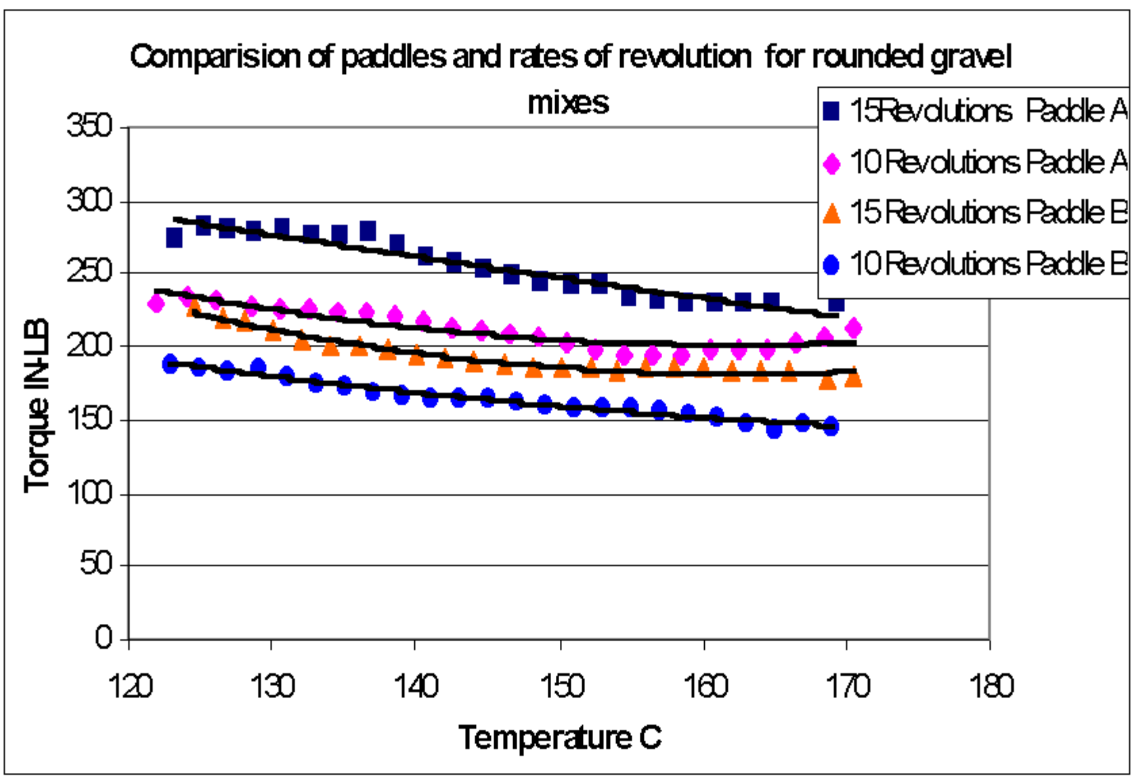

Figure 24. Comparison of Paddles and Rates of Revolution for Rounded Gravel Mixes

For all three mixes, Paddle A typically provided a wider range in torque values when compared to Paddle B. Also, the 15 RPM rotational speed typically generated a wider range in torque values than the 10 RPMs. Therefore, the combination of Paddle A and 15 RPMs was fixed for the remaining of the study.

Calibrating the Device

Before the start of additional testing, a method was developed to check the calibration of the workability equipment. Since the equipment was in the development process there was no ready-made calibration device available. So, in order to calibrate the device, granite aggregate passing the 1.18 mm sieve (No. 16) and retained on 0.60 mm (No. 30) sieve weighing 20-kilogram was tested in the workability device. The torque values obtained varied between 172 and 175 in-lb. This aggregate was made the standard and the device was run with this aggregate after every 10 tests to ensure calibration.

Effect of Mix Constituents on Workability

Tests were conducted utilizing the refined workability device on mixes containing various combinations of aggregate type (granite, limestone, and crushed gravel), gradation shape (ARZ and BRZ), nominal maximum aggregate size (12.5 and 19.0 mm), and binders (PG 64-22, PG 70-22, and PG 76-22). Testing of these various mixes was conducted to evaluate the effect of mix characteristics on workability. Two replicates of each mix were tested.

To analyze the data, torque values were determined for each mix at 120, 130, 140, 150, 160, and 170ºC. The regression lines (exponential model) described previously were used to determine the average torque at each temperature. Tables 8, 9, and 10 provide the average torque values for mixes containing the granite, limestone, and crushed gravel aggregates, respectively. Raw data is provided in Appendix A.

Based on the data presented in Tables 8, 9, and 10, there were obvious effects of aggregate type, binder type, and temperature. Collectively, mixes containing the crushed gravel had a much lower torque value (more workable) than mixes containing the granite and limestone aggregates at a given temperature. On average, mixes containing the crushed gravel aggregate produced approximately 55 in-lbs less torque than the granite and limestone mixes (Figure 25). Mixes containing the PG 76-22 binder produced much higher torques than mixes containing the PG 64-22 and PG 70-22 binders (Figure 26). Interestingly, mixes containing the PG 64-22 and PG 70-22 binders had similar torque values. As expected, there was a large impact of temperature on the workability of mixes (Figure 27), as temperature decreased, torque values increased.

Analysis of the torque data was conducted using an analysis of variance (ANOVA). Factors included in the ANOVA were aggregate type, NMAS, gradation shape, binder type, and test temperature. Results of the ANOVA are presented in Table 11.

Table 8. Average Torque Values for Mixes Containing Granite Aggregates

NMAS	Gradation	Binder	Torque (in-lb) at Temperature 120 C	130 C	140 C	150 C	160 C	170 C
12.5	ARZ	PG 64-22	300	275	253	232	212	195
		PG 70-22	309	280	254	230	208	189
		PG 76-22	401	365	332	302	275	250
	BRZ	PG 64-22	296	273	251	232	213	196
		PG 70-22	290	261	236	212	191	172
		PG 76-22	462	409	362	320	283	251
19.0	ARZ	PG 64-22	348	325	304	284	265	248
		PG 70-22	333	304	277	252	229	209
		PG 76-22	409	383	359	336	315	295
	BRZ	PG 64-22	336	308	282	259	237	217
		PG 70-22	320	293	268	246	226	207
		PG 76-22	367	333	302	274	248	225

Table 9. Average Torque Values for Mixes Containing Limestone Aggregates

NMAS	Gradation	Binder	Torque (in-lb) at Temperature 120 C	130 C	140 C	150 C	160 C	170 C
12.5	ARZ	PG 64-22	262	243	225	209	194	180
		PG 70-22	274	254	234	217	201	186
		PG 76-22	363	333	306	281	258	237
	BRZ	PG 64-22	279	255	233	213	195	178
		PG 70-22	318	281	248	219	193	171
		PG 76-22	466	402	348	300	259	224
19.0	ARZ	PG 64-22	339	313	289	266	245	226
		PG 70-22	331	303	278	255	234	215
		PG 76-22	389	368	347	328	310	293
	BRZ	PG 64-22	305	272	243	217	194	173
		PG 70-22	372	323	281	244	212	184
		PG 76-22	543	454	380	317	265	222

Table 10. Average Torque Values for Mixes Containing Crushed Gravel Aggregates

NMAS	Gradation	Binder	Torque (in-lb) at Temperature 120 C	130 C	140 C	150 C	160 C	170 C
12.5	ARZ	PG 64-22	225	208	191	176	163	151
		PG 70-22	239	218	198	181	165	150
		PG 76-22	298	272	249	227	208	190
	BRZ	PG 64-22	222	207	193	179	167	155
		PG 70-22	258	236	215	197	179	164
		PG 76-22	347	309	275	245	219	195
19.0	ARZ	PG 64-22	289	263	240	219	199	181
		PG 70-22	259	238	218	201	184	169
		PG 76-22	320	293	268	245	224	205
	BRZ	PG 64-22	246	231	216	203	190	178
		PG 70-22	285	257	232	209	189	170
		PG 76-22	363	324	289	258	230	206

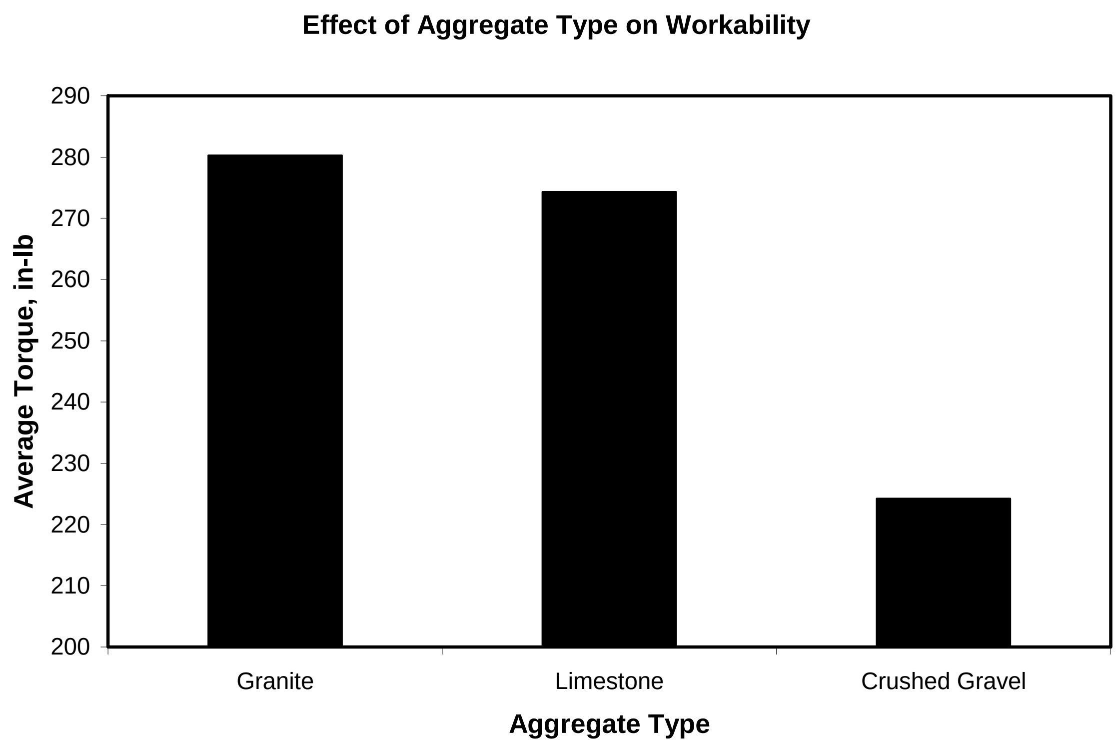

Figure 25. Effect of Aggregate Type on Workability

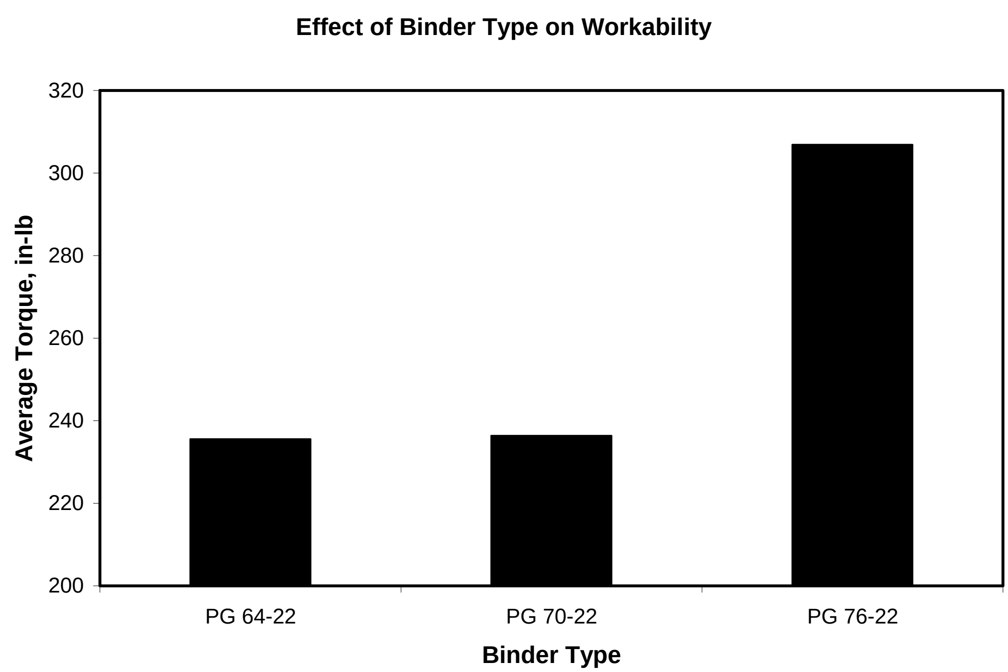

Figure 26. Effect of Binder Type on Workability

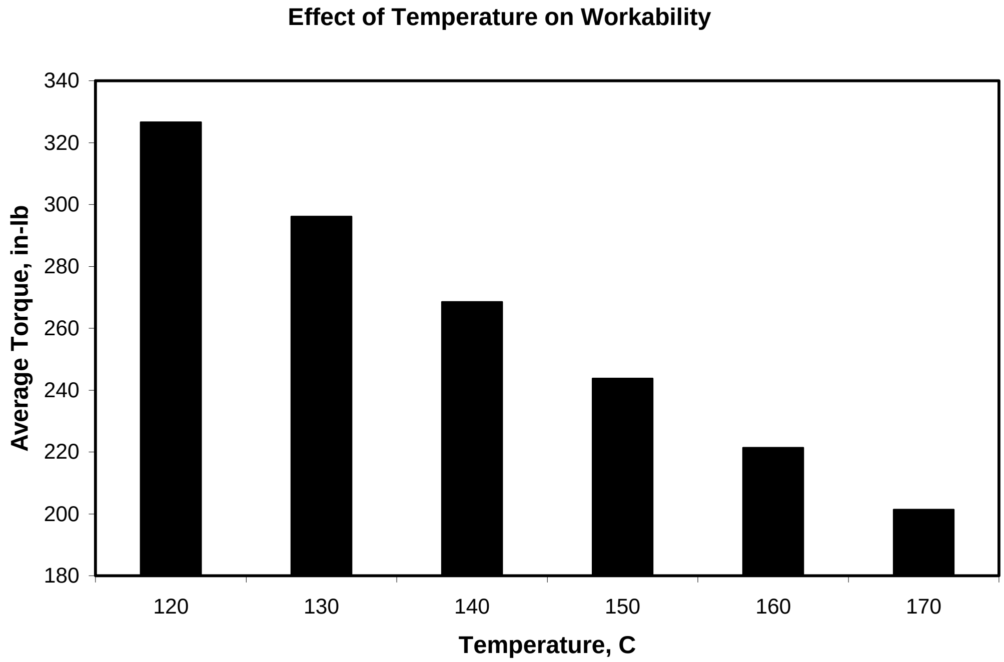

Figure 27. Effect of Mix Temperature on Workability

Based on the ANOVA, all of the main factors except gradation shape had a significant effect on workability. Binder type had the largest effect as shown by the highest F-statistic (1226.79). The factor with the next largest effect was test temperature, followed by aggregate type, and NMAS, respectively. An interesting observation about Table 11 was that a very large number of two-, three-, and four-way interactions were also significant. Also of interest in Table 11 are the mean squares for the error (196). This value is equal to the repeatability variance. By taking the square root of this value, the repeatability standard deviation can be obtained (14 in-lbs). This value is relatively small compared to the magnitude of torque values obtained during testing (as will be shown). Below are discussions on the results of the ANOVA.

Effect of Aggregate Type

Table 11 showed that there was a significant effect of aggregate type on workability (torque). The overall effect of aggregate type was illustrated in Figure 25. A Duncan's Multiple Range Test (DMRT) showed that the granite and limestone aggregates provided similar torque values and mixes utilizing the crushed gravel aggregate had significantly lower torque values (Table 12). These results were not unexpected. Both the granite and limestone aggregates are quarried and have 100 percent fractured faces. Table 4 showed that the crushed gravel aggregate only had 80 percent fractured faces (two faces). This confirms that angular, crushed aggregates reduce the workability of HMA mixes.

Table 11. Results of ANOVA on Torque Data

Source	DF	MS	F-statistic	F-critical (α=0.05)	P-value	Significant (α=0.05)?
Aggregate Type (Agg)	2	136337	694.09	3.00	0.000	Yes
NMAS	1	70789	360.39	3.84	0.000	Yes
Gradation Shape (Grad)	1	11	0.05	3.84	0.816	No
Binder Type (Bind)	2	240973	1226.79	3.00	0.000	Yes
Temperature (Temp)	5	158264	805.72	2.21	0.000	Yes
Agg*NMAS	2	3067	15.61	3.00	0.000	Yes
Agg*Grad	2	5153	26.23	3.00	0.000	Yes
Agg*Bind	4	6657	33.89	2.37	0.000	Yes
Agg*Temp	10	1564	7.96	1.83	0.000	Yes
NMAS*Grad	1	13804	70.28	3.84	0.000	Yes
NMAS*Bind	2	5164	26.29	3.00	0.000	Yes
NMAS*Temp	5	187	0.95	2.21	0.449	No
Grad*Bind	2	6259	31.87	3.00	0.000	Yes
Grad*Temp	5	3495	17.79	2.21	0.000	Yes
Bind*Temp	10	3629	18.47	1.83	0.000	Yes
Agg*NMAS*Grad	2	1086	5.53	3.00	0.005	Yes
Agg*NMAS*Bind	4	2932	14.92	2.37	0.000	Yes
Agg*NMAS*Temp	10	456	2.32	1.83	0.013	Yes
Agg*Grad*Bind	4	2369	12.06	2.21	0.000	Yes
Agg*Grad*Temp	10	1447	7.37	1.83	0.000	Yes
Agg*Bind*Temp	20	144	0.73	1.57	0.791	No
NMAS*Grad*Binder	2	3098	15.77	3.00	0.000	Yes
NMAS*Grad*Temp	5	63	0.32	2.21	0.899	No
NMAS*Bind*Temp	10	163	0.83	1.83	0.599	No
Grad*Bind*Temp	10	1633	8.31	1.83	0.000	Yes
Agg*NMAS*Grad*Bind	4	3049	15.52	2.37	0.000	Yes
Agg*NMAS*Grad*Temp	10	151	0.77	1.83	0.660	No
Agg*NMAS*Bind*Temp	20	75	0.38	1.57	0.993	No
Agg*Grad*Bind*Temp	20	288	1.47	1.57	0.096	No
NMAS*Grad*Bind*Temp	10	40	0.20	1.83	0.996	No
Agg*NMAS*Grad*Bind*Temp	20	156	0.80	1.57	0.717	No
Error	216	196	---	---	---	---

Table 12. DMRT Rankings for Aggregate Type

Aggregate Type	Mean Torque Value (in-lb)	DMRT Rankings*
Granite	280	A
Limestone	274	A
Crushed Gravel	224	B

* Means with different letter rankings are significantly different.

Table 11 showed that there were significant two-way interactions between aggregate type and all of the other main factors (NMAS, gradation shape, binder content, and temperature). The interactions between the aggregate type and the other factors are illustrated in Figures 28 through 31. Figure 28 shows that for the 12.5 mm NMAS, mixes containing the granite aggregate had the highest torque values, followed by the limestone mixes and crushed gravel mixes, respectively. However, for the 19.0 mm NMAS mixes, torque values were approximately the same for the limestone and granite mixes and were much higher than the crushed gravel mixes.

Figure 29 shows that for the finer gradation (ARZ), mixes containing the granite aggregate provided higher torque values than the limestone and crushed gravel mixes. However, for the coarse gradations (BRZ), both the granite and limestone mixes yielded similar torque values that were much higher than the crushed gravel mixes. Interestingly, both the limestone and crushed gravel mixes had similar workability (similar torque values) characteristics for both gradation shapes, while the granite mixes, having the finer gradation, were less workable than the coarse mixes.

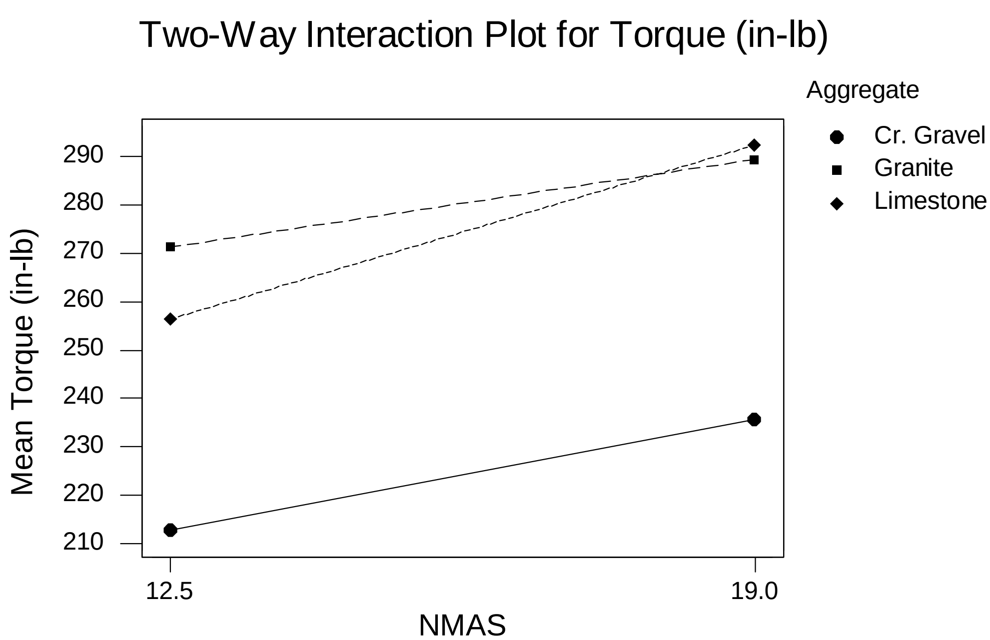

Figure 28. Interaction Between Aggregate Type and NMAS

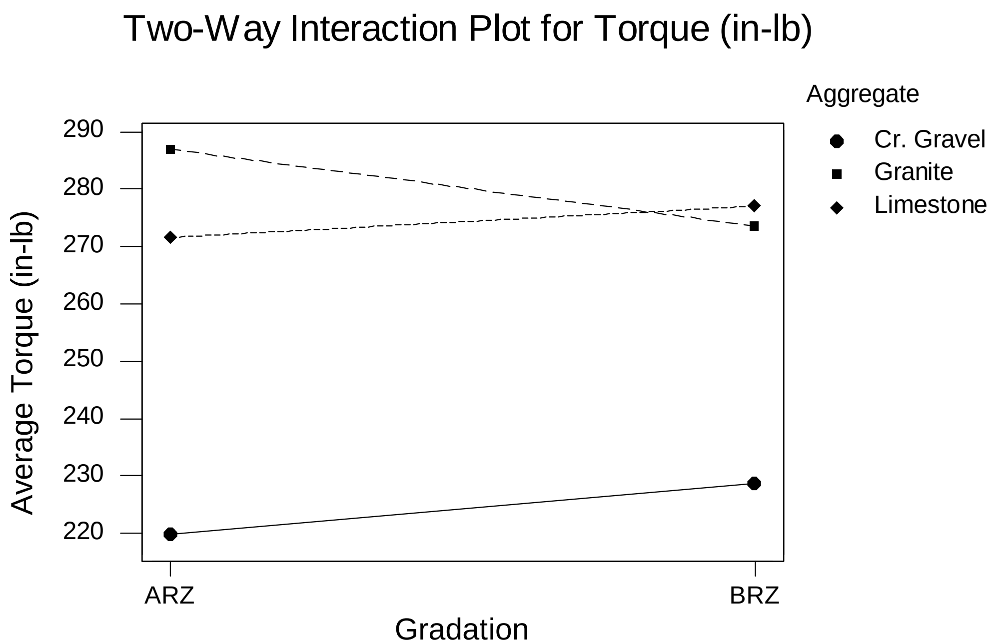

Figure 29. Interaction Between Aggregate Type and Gradation Shape

Figure 30 illustrates the interaction between aggregate type and binder type. For all three aggregate types, the workability was relatively consistent for mixes containing both the PG 64-22 and PG 70-22 binders. For mixes containing the PG 64-22 binder, there was a relatively large difference in average torque values for the granite and limestone mixes. However, for the mixes containing PG 70-22 and PG 76-22 binder, torque values were basically the same for mixes containing the granite and limestone aggregates. Another interesting observation was that crushed gravel mixes combined with the PG 76-22 binder had a similar workability as the granite and limestone mixes combined with either the PG 64-22 or PG 70-22.

Figure 31 illustrates the interaction between aggregate type and test temperature. At the lower temperatures (120 to 140ºC), the generated torque values for the mixes containing the granite and limestone aggregates were approximately the same. However, at the higher temperatures, the granite mixes became less workable.

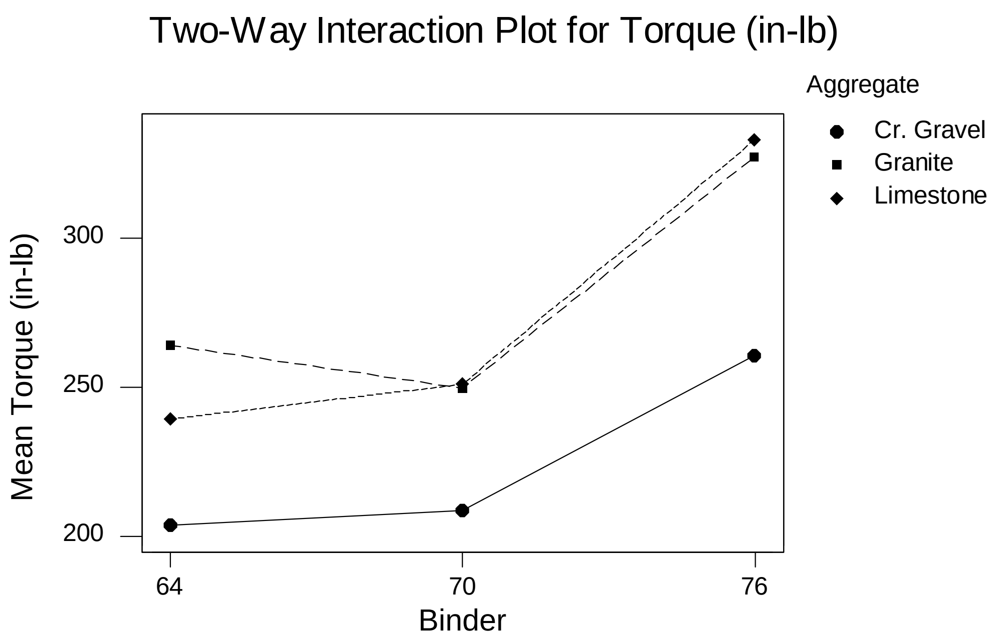

Figure 30. Interaction Between Aggregate Type and Binder Type

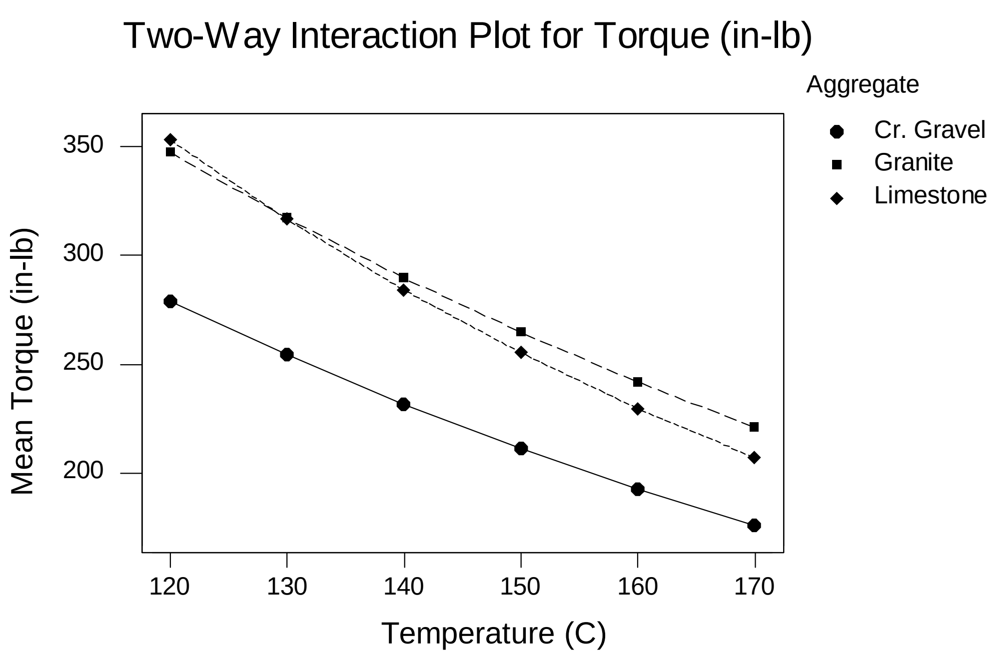

Figure 31. Interaction Between Aggregate Type and Temperature

Effect of NMAS

The next factor shown to be significant in Table 11 was NMAS. Figure 32 shows the effect of NMAS on workability (torque). Based on this figure, mixes having a 19.0 mm NMAS generated more torque (less workable) than the 12.5 mm NMAS mixes. Since there were only two levels of NMAS, a DMRT was not needed. Based upon the significance of NMAS shown in Table 10 and the data illustrated in Figure 32, it can be concluded that mixes having a 19.0 mm NMAS are less workable than mixes having a 12.5 mm NMAS. Table 11 also showed that the two-way interactions between NMAS and both gradation and binder type were significant. Figure 32 illustrates the two-way interaction between NMAS and gradation shape. This figure shows that the difference in torque between the two NMAS mixes is greater for the fine-graded mixes (ARZ) than for the coarse-graded mixes (BRZ). The figure also shows that the torque is approximately the same for the 19.0 mm NMAS mixes no matter the gradation shape. However, for the 12.5 mm NMAS mixes, the coarser gradations are less workable (higher average torque values).

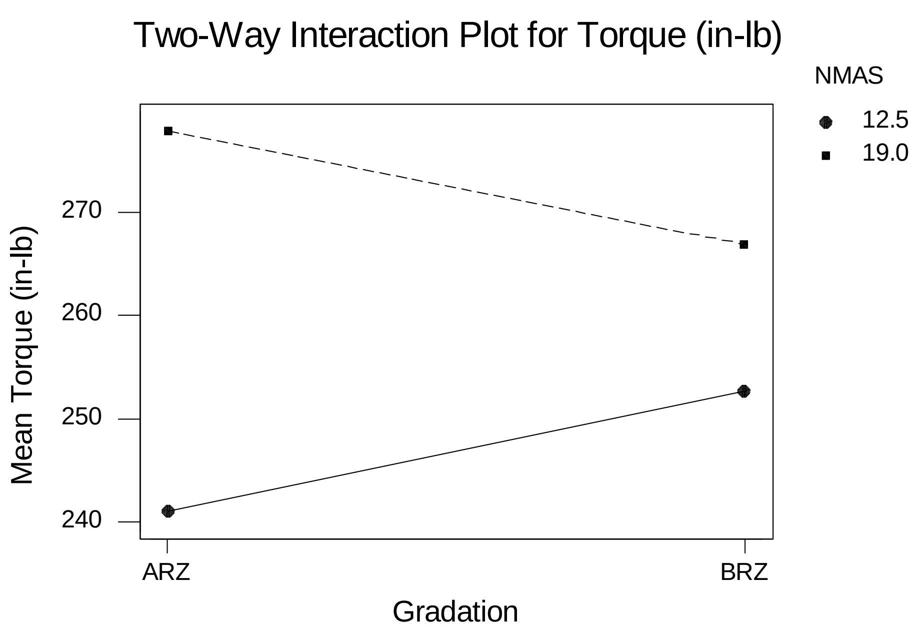

Figure 32. Interaction Between NMAS and Gradation Shape

Figure 33 shows the interaction between NMAS and binder type. Based on this figure, there was a greater difference in torque between the two NMAS mixes containing the PG 64-22 than for mixes containing the PG 76-22. This would suggest that NMAS has a greater influence on workability when unmodified binders are utilized.

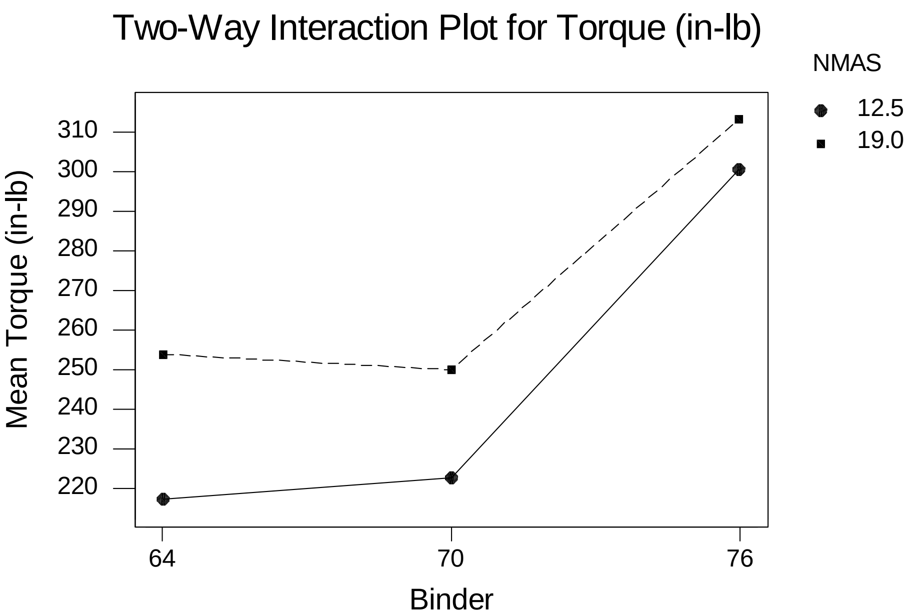

Figure 33. Interaction Between NMAS and Binder Type

Effect of Binder Type

The next factor identified in Table 11 as having a significant effect on workability was binder type. Figure 26 illustrated this effect. A DMRT analysis was conducted to evaluate the significant differences between the different binders (Table 13). Based on this table, mixes containing the PG 76-22 binder had significantly higher torque values than mixes with both the PG 70-22 and PG 64-22 binders. Interestingly, there were no differences between the PG 70-22 and PG 64-22 mixes.

Table 13. DMRT Rankings for Binder Type

Aggregate Type	Mean Torque Value (in-lb)	DMRT Rankings*
PG 76-22	307	A
PG 70-22	236	B
PG 64-22	236	B

* Means with different letter rankings are significantly different.

Table 7 showed that there were differences between the three binders based in the Superpave binder testing protocols. Both the PG 70-22 and the PG 76-22 binders were polymer-modified. Results in Table 13 suggest that there may be a level of modification below which the workability of a mixture is not affected. However, if the modification is above some level, the workability of a mixture is greatly reduced.

Based on Table 11, there was a two-way interaction between binder grade and test temperature. This interaction is illustrated in Figure 34. Based on this figure, the mixes containing the PG 64-

22 and PG 70-22 had similar workability characteristics, both in magnitude and slope. However, the mixes containing the PG 76-22 binder were less workable (higher torque values) and were more affected by temperature (steeper slope).

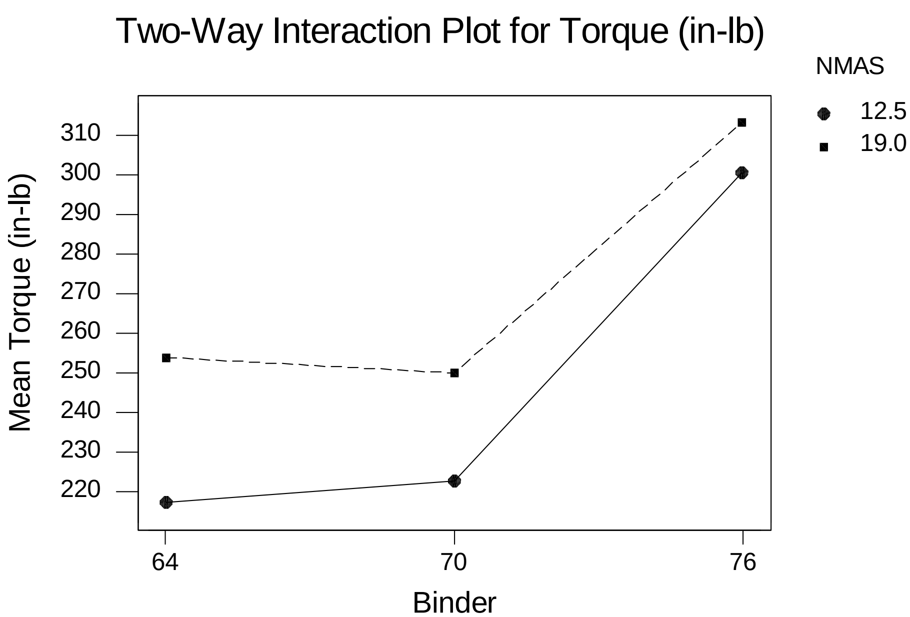

Figure 34. Interaction Between Binder Type and Temperature

Effect of Temperature

The last factor shown to significantly affect torque values was temperature. This was expected. Past experiences have shown that mixes become harsher and less workable at lower temperatures. The effect of temperature on workability was shown in Figure 27.

Summary of Workability Testing

Results of the workability testing showed that the prototype equipment can determine the workability characteristics of HMA. Based upon the test results, workability was affected by aggregate type, NMAS, binder type, and temperature. Interestingly, workability was not significantly affected by gradation shape. However, Figure 32 showed that gradation shape has more of an affect for 12.5 mm NMAS gradations than 19.0 mm NMAS mixes. Table 11 showed that there were a number of two- and three-way interactions that significantly affected workability. Therefore, it appears that different HMA mixes exhibit different workability characteristics.

Concept of Using Mix Workability To Define Compaction Temperature of HMA Mixes

During the initial stages of the development of the workability test, the torque values generated were generally constant or increased only slightly when the temperature decreased from 170°C. However, after reaching a certain temperature the torque values began to increase significantly. The rate of increase in torque was relatively lower for the PG 64-22 and PG 70-22 binders, but as the level of modification increased to a PG 76-22, the rate of increase was higher (Figure 35). Therefore, the general trend of the workability curve is similar to the viscosity-temperature curves for the different binders shown in Figure 10. However, the magnitude of the workability curve was governed not only by the viscosity of the binder but the properties of the aggregates and NMAS as well. This can be seen from Figures 35, 36, and 37. Figure 35 shows a comparison of workability for two mixes with the same binder (PG 64-22), gradation (ARZ), and NMAS (12.5mm), but different aggregate types. This figure shows that even though the same binder was used for the three mixes each mix had different workabilities due to the difference in aggregate type (and, thus, properties).

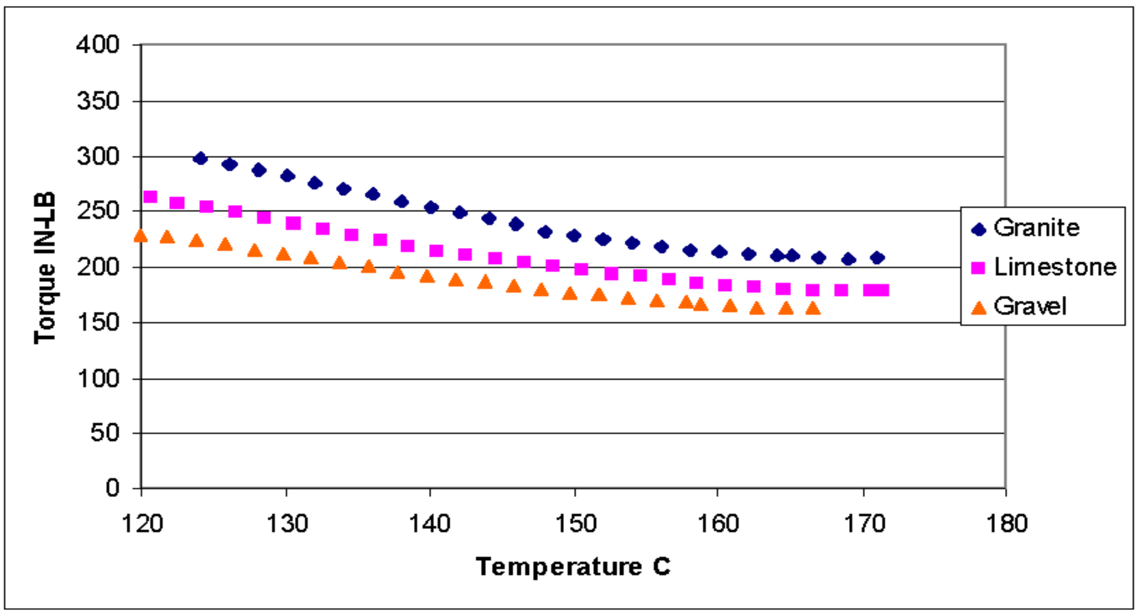

Figure 35. Workability Curves for Same Mixes with Different Aggregates (PG 64-22, ARZ, 12.5mm NMAS).

The use of workability to determine compaction temperature was investigated. Figure 36 shows comparison between workabilites of two mixes with the same binder (PG 64-22), NMAS (19mm), and type of aggregate (limestone) but with varying gradations. In spite of the similarity in the binder, the mix workability was different.

Figure 37 shows a comparison between workabilities of two mixes with, the same binder (PG 76-22), type of aggregate (limestone) and gradation (ARZ) but with varying NMAS. The presence of larger particles in the 19.0 mm NMAS mix increased the torque necessary to work the mix at a given temperature. For this reason the workability was less for mixes with larger NMAS.

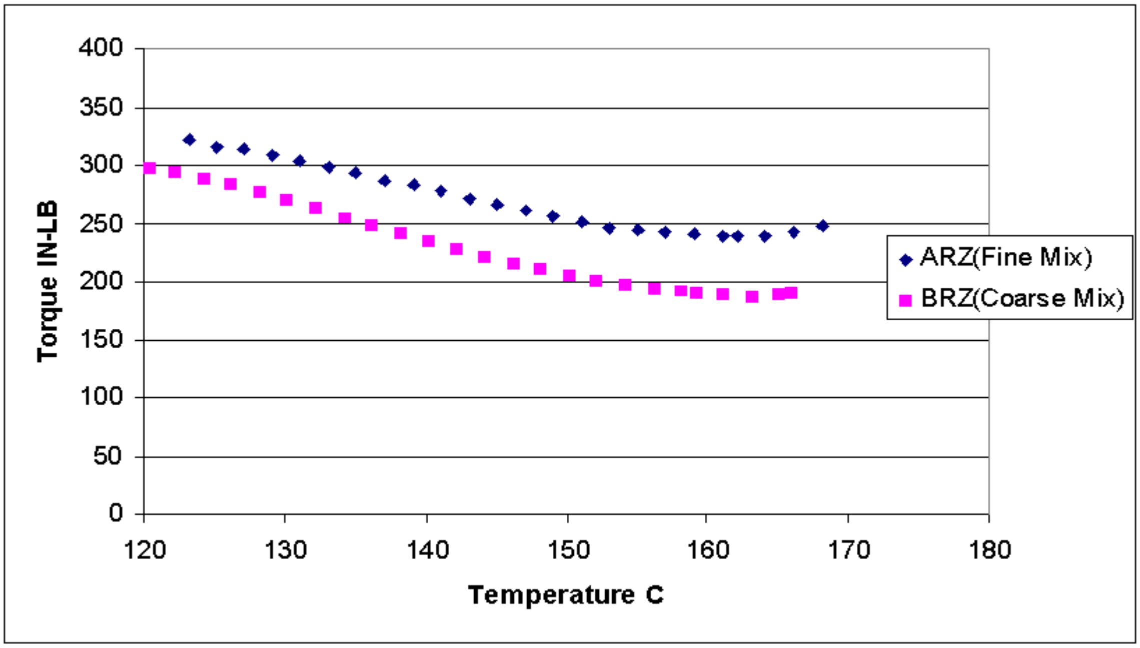

Figure 36. Workability Curves for Same Mixes with Different Gradations (PG 64-22, 19mm NMAS, Limestone).

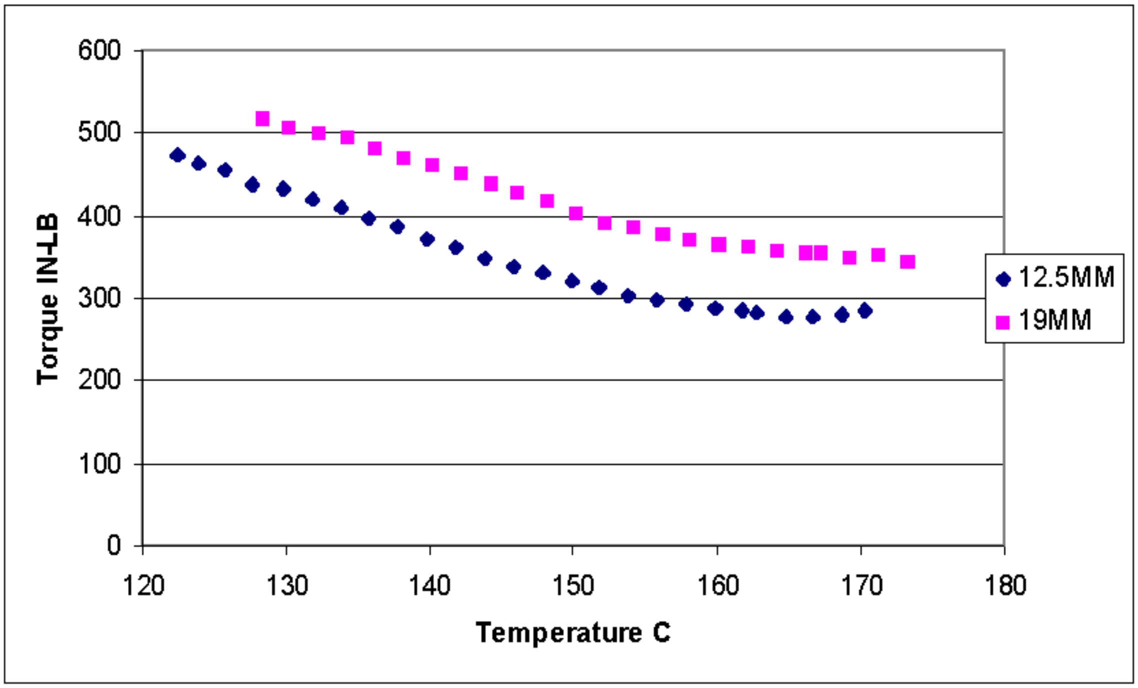

Figure 37. Workability Curves for Same Mixes with Different Nominal Maximum Aggregate Sizes (PG 76-22, ARZ, Limestone).

Compacting Temperature Methodology

From Figures 35 to 37 it can be inferred that the general shape of the workability curve depends on the change in binder viscosity with temperature whereas the magnitude of the workability curve depends both on binder viscosity and the aggregate properties of the mix. The initial concept in developing a mixture's compaction temperature was based on equi-stiffness (workability). However, within the temperature range tested it was determined that mixes containing the PG 76-22 always had a temperature much higher (if it could be determined) than the other binder types. Therefore, that approach was abandoned.

One of the requirements of compaction temperature in the field is to get proper workability of the mix while compacting. Keeping this as a priority, the temperature on the workability curve from which the torque begins to increase dramatically was taken as the lowest desirable compaction temperature. Compaction temperatures suggested by this method take into account the viscosity of the binder as well as properties of the mix constituents.

Compaction temperatures were initially established for all the mixes as the temperature where the mix workability began stabilizing. Straight lines were drawn on the workability curve to establish a temperature. Compaction temperature obtained by this method seemed to be a slightly different for different aggregate variations. However, since the aggregates also have an effect on the mix viscosity, this seems reasonable. Compaction temperatures found by this method for all the mixes and the compaction temperatures by the traditional method are shown in the Table 14.

It can be seen from Table 14 that the compaction temperatures obtained through the workability measurements for mixes containing the PG 64-22 were similar to those obtained by the traditional method (temperature-viscosity). However, for the PG 70-22 and PG 76-22 binders, the compaction temperatures were lower when compared to the traditional method. For mixes with the PG 70-22 binder, the compaction temperatures are lower by 9 to 17° C; whereas, for PG 76-22 the compaction temperatures were lower by 16 to 28° C when using the workability results. Since the PG 70-22 was not as modified, the lower compaction temperatures than for the PG 76-22 mixes seem logical.

Shear Study

To validate the workability compaction temperatures, mixes were compacted using a SGC at three different temperatures. The SGC used in this study has the capability to measure the power required to keep the mold rotating at an angle of 1.25° and convert this value of power into shear. Mixes were compacted at the workability established compaction temperature and 15°C above and 15°C below the compaction temperatures (Figure 38).

The shear study was conducted on selected mixes. Samples were compacted to 100 gyrations. The maximum shear ratio obtained for a particular temperature was plotted with the maximum shear ratio obtained at other temperatures for the same type of mix (Figure 39). The shear tests were conducted on the mixes shown in Table 15.

Table 14. Compaction Temperatures

Mix type*	Compaction Temperature by traditional Method ° C			Compaction Temperature by the current study Method ° C		
	64-22	70-22	76-22	64-22	70-22	76-22
12.5AGR	149	164	179	152	155	157
12.5BGR				147	147	156
19AGR				155	------	163
19BGR				152	------	157
12.5ACG				155	155	155
12.5BCG				141	148	151
19ACG				151	151	156
19BCG				148	155	157
12.5ALMS				150	150	154
12.5BLMS				147	150	156
19ALMS				153	153	155
19BLMS				152	153	159

**Designation: The first number indicate NMAS, the second letter indicates the gradation, and the remaining letters indicate the type of aggregate*

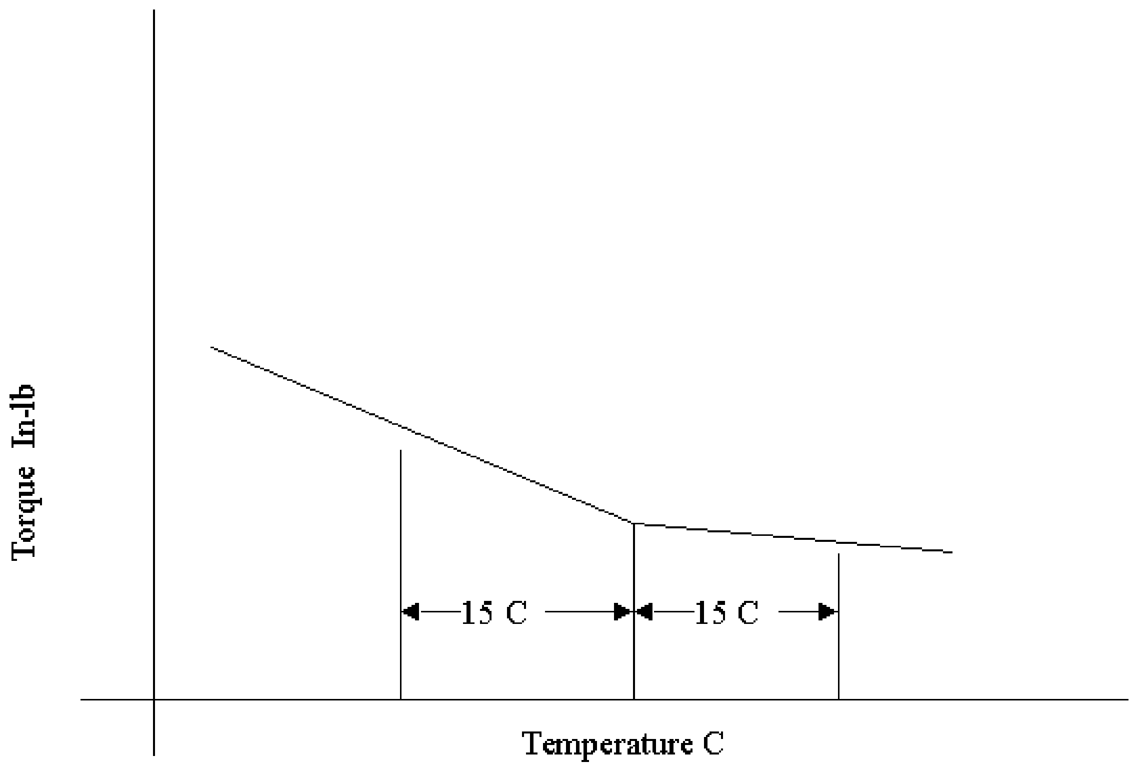

Figure 38. Samples Compacted at 15 Degree Increments (Shear Study)

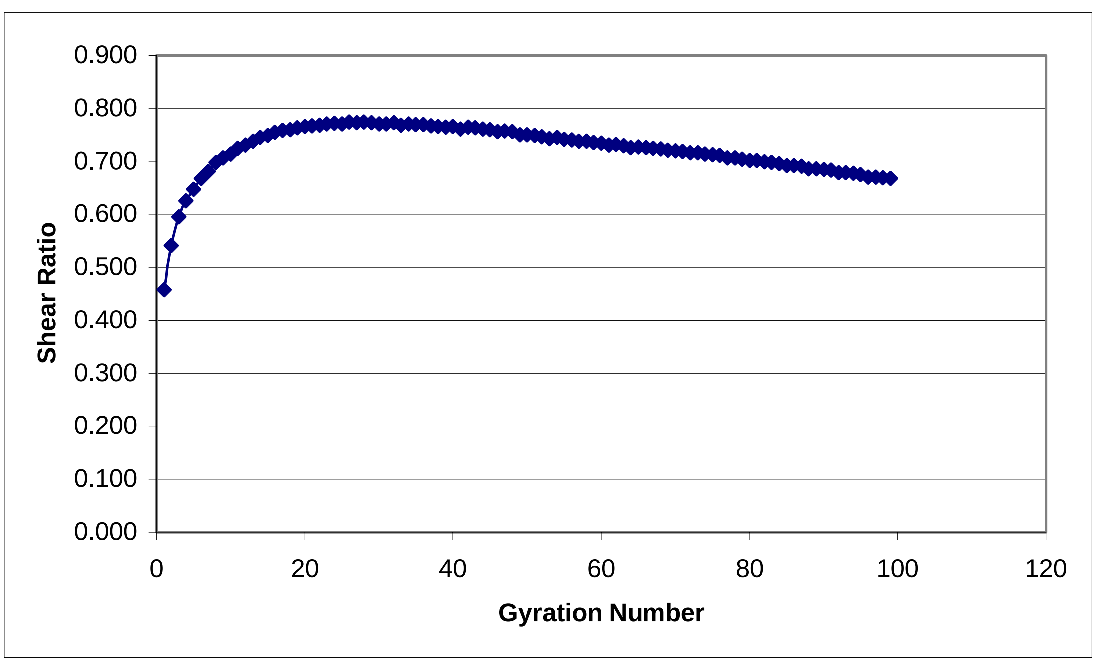

Figure 39. Typical Gyration Versus Shear Ratio Obtained from the Gyratory Compactor

Table 15. Samples Tested in the Shear Study

Mix Designation *
19BRZGRAN
12ARZLMS
12BRZLMS

**Designation: The first number indicate NMAS, the second letter indicate the gradation the remaining letters indicate the type of aggregate.*

The variation in shear ratio values with temperature for the tested mixes can be seen in Figures 40, 41, and 42. The results of shear ratio with temperature did not provide any definite trend. This may be because the number of samples tested was too small or the SGC was not sensitive enough to measure change in mix characteristics with temperature.

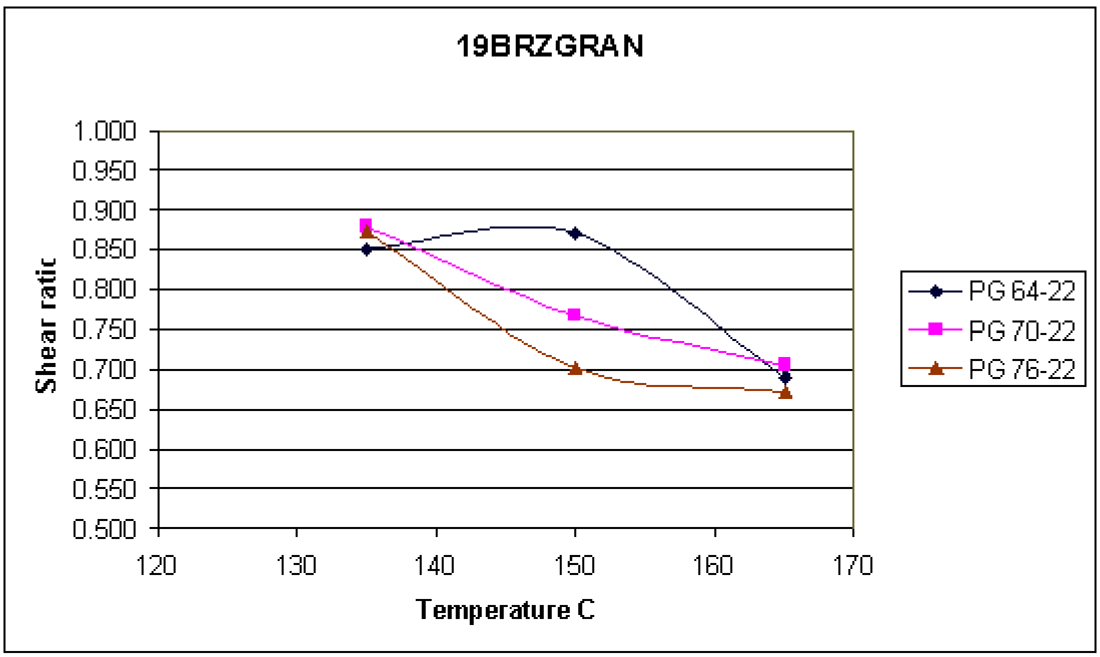

Figure 40. Shear Study Results for 19BRZGRAN Mixes with Different Binder

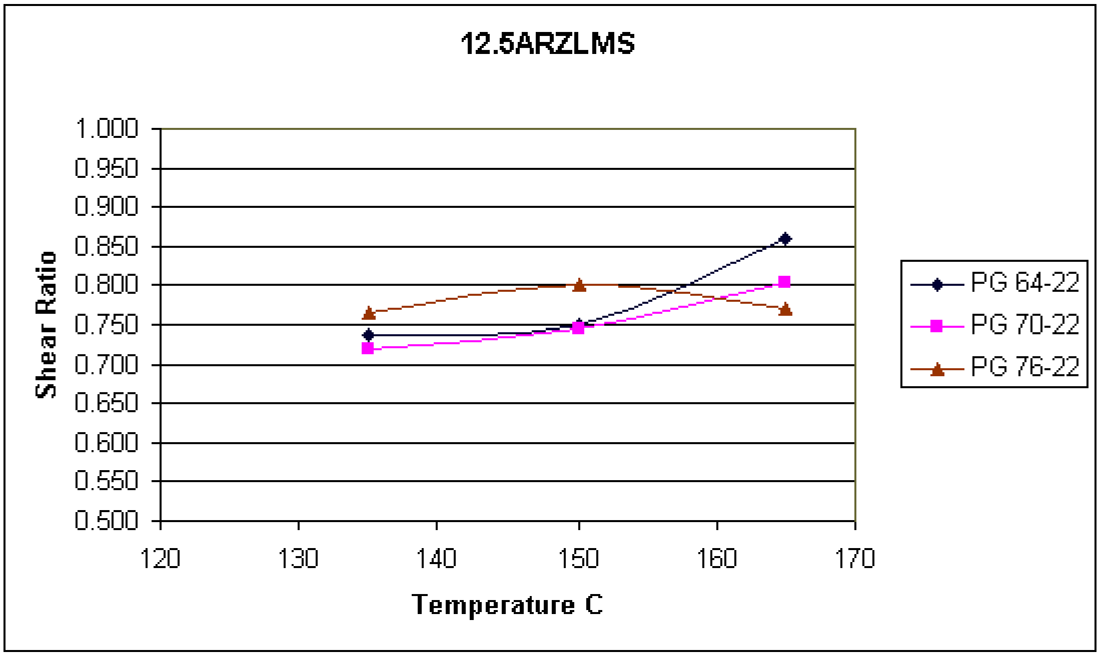

Figure 41. Shear Study Results for 12.5ARZLMS Mixes with Different Binder

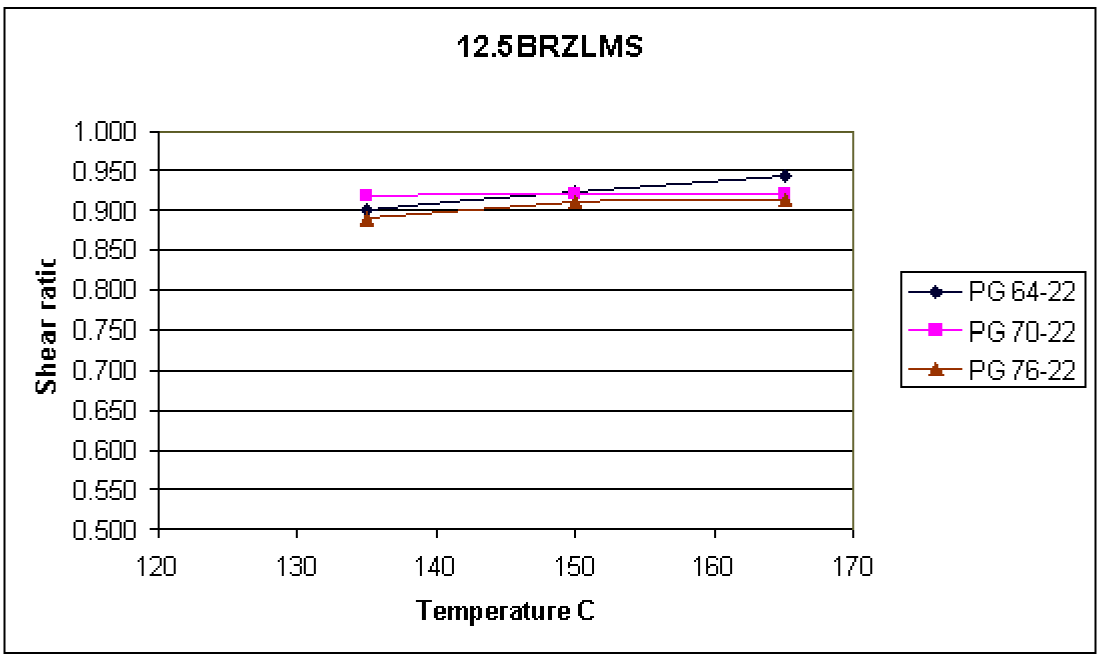

Figure 42. Shear Study Results for 12.5BRZLMS Mixes with Different Binder

Based on recent research reported, subsequent to the beginning of this study, by the Asphalt Institute *(16),* the outcome of the gyratory shear experiment was not surprising. Within their research, gyratory shear results were compared to the rutting potential of mixes. However, during the course of the work, it was shown that gyratory shear was not sensitive to binder grade. Therefore, the gyratory shear ratio was not sensitive to the viscosity of binders as temperatures were changed.

CONCLUSIONS AND RECOMMENDATIONS

The primary objective of this study was to develop a device to measure the workability of hot mix asphalt (HMA) mixes. Workability was used in this study to describe the ease with which a HMA could be constructed. The workability of mixes was evaluated by pushing a paddle through HMA and measuring the torque required to maintain a given rate of revolution. Based on the test results and analyses conducted in this study, the following conclusions are provided:

- A device was successfully designed to measure the laboratory workability of HMA mixes.
- The workability of HMA as measured by the device was affected by aggregate type, and, thus, aggregate properties. Mixes prepared with a cubical, angular granite were less workable (generated more torque at a given temperature) than mixes prepared with a semi-angular crushed gravel.
- The workability of HMA as measured by the device was affected by the nominal maximum aggregate size (NMAS) of the gradation. As NMAS increased for a given aggregate type, gradation shape, and binder type, workability decreased.
- Gradation shape did not have a significant effect on workability. However, there were numerous two- and three-way interactions which were significant that included gradation shape.
- Binder type significantly affected the workability of mixes. As expected, mixes modified to meet a PG 76-22 were significantly less workable than mixes containing an unmodified PG 64-22 for a given temperature.
- As expected, the temperature of the mix significantly affected the workability of HMA. There was a relationship between workability and temperature that showed increased workability at higher temperatures.
- A preliminary attempt was made at utilizing workability data to determine a realistic compaction temperature of HMA mixes. However, this was a limited effort and the results were inconclusive.

One of the important issues in the HMA industry is the compactibility of mixes. This concern has become more pronounced due to the increased use of coarse-graded mixes and/or the increased use of polymer-modified binders (mixes with low workability). Compactibility of HMA is related to workability; therefore, the conclusions of this study were important in that the workability of HMA mixes was successfully characterized and that the prototype device could differentiate between different mix characteristics. Since the workability of HMA mixes can be measured, future work should be conducted to develop the relationship between workability and compactibility.

Prior to future research with the workability device, there should be some minor refinements of the prototype device. Specific areas needing refinement include the design of the paddle and sample container to minimize the amount of aggregates being caught between the paddle and container side. A next generation device should also include an additional temperature sensor to provide a better measure of temperature. The data acquisition system should also be enhanced prior to additional study with the device. The prototype acquisition system output 48 data points per second. The next generation device should be able to better average results to minimize noise within the data. Finally, re-engineering of the equipment is needed to make the device more user friendly.

Testing within future research should involve mixes with a wide range in compactibility. Field produced HMA mixture should be tested in the workability device and then the compactibility in the field monitored. Monitoring of compactibility would entail fully documenting mix properties, thickness, and roller types/patterns along with mat temperature. Changes in density between roller passes should also be monitored using a nondestructive method to evaluate relative changes in density.

The relationship between compactibility and workability for the field mixes would likely result in guidance on the difficulty of compacting a particular mix on the roadway. As an example, four ranges of stiffness (workability) could be developed to provide guidance on the field compactive effort needed to achieve a desirable density (Table 16). Both temperature and stiffness would be tied to the guidance provided. As shown within this study, a given mix has a relationship between stiffness and temperature. If a particular mix had a given stiffness at 140°C and was categorized as difficult to achieve a desirable density, then at 150°C the stiffness might be such that it would fall in the “normal compactibility” category. Therefore, by increasing the temperature of the mix by 10°C on the roadway, additional rollers would not be necessary to achieve a desirable density. Development of guidance categories similar to that shown in Table 16 could be a great benefit to the HMA industry.

Table 16. Possible Guidance for Compactibility Using the Workability Device

Compactibility Category	Workability Values (torque)	Comments
Easy	TBD	Mixes falling in this category could be easily placed and compacted on the roadway. These mixes may also show tenderness on the roadway and may slump in trucks during transportation.
Normal	TBD	Mixes in this category would be reasonably easy to place and compact using typical roller types and rolling patterns.
Difficult	TBD	Mixes falling in this category would be difficult to place and compact in the field. Handwork would also be difficult. Either the number of rollers or the size of the rollers would need to be increased to achieve density.
Very Difficult	TBD	Mixes in this category would be very difficult to produce, place, and compact. Handwork would be near impossible. The size and/or number of rollers would likely be needed to achieve density.

TBD – To be determined through future research.

REFERENCES

1. Roberts, F. L., P. S. Kandhal, E. R. Brown, D. Y. Lee, and T. W. Kennedy. Hot Mix Asphalt Materials, Mixture Design, and Construction. NAPA Education Foundation, Second Edition. Lanham, Maryland. 1996.

2. The Asphalt Handbook. Manual Series No. 4 (MS-4). Asphalt Institute. Lexington, Kentucky. 1989.

3. Terrel, R. L., J. A. Epps, and C. Crawford. Making the Most of Temperature, Viscosity Characteristics. Information Series 102. NAPA. Lanham, Maryland. 1988.

4. Marvillet, J. and P. Bougalt. Workability of Bituminous Mixes. Development of a Workability Meter. Proceedings, Association of Asphalt Paving technologists. Volume 48. Denver, Colorado. 1979.

5. Tattersol, G. H. and P. G. G. Banfill. A New Rheometer For Soft-to-Fluid Fresh Concrete. American concrete Institute Materials Journal. Volume 96, Issue 1, 1999.

6. Bahia, H. U., W. P. Hislop, H. Zhai, and A. Rangel. Classification of Asphalt Binders into Simple and Complex Binders. Journal of the Association of Asphalt Paving Technologists. Boston, Massachusetts. 1998.

7. Hensley, J. and A. Palmer. Establishing Hot Mix Asphalt Mixing and Compaction Temperatures At the Project Level. http://www.asphaltinstitute.org/superpav/temperature/html. Asphalt Institute. September 20, 2002

8. Watson, D. E. An Updated Review of SMA and Superpave Projects. Paper Submitted For Presentation and Publication at the 2003 Annual Meeting of the Transportation Research Board. Washington, D. C. January 2003.

9. Mix Design Methods for Asphalt Concrete and Other Hot-Mix Types. Manual Series No. 1. Asphalt Institute. 1962.

10. Mix Design Methods for Asphalt Concrete and Other Hot-Mix Types. Manual Series No. 2. Asphalt Institute. 1974.

11. Yildrim, Y., M. Solaimanian, and T. Kennedy. Mixing and Compaction Temperatures for Superpave Mixes. Journal of the Association of Asphalt Paving Technologists. Vol. 69. Reno, Nevada. 2000.

12. DeSombre, R., D. E. Newcomb, B. Chadbourn, and V. Voller. Parameters to Define the Laboratory Compaction Temperature Range of Hot Mix Asphalt. Journal of the Association of Asphalt Paving Technologists. Volume 67, Boston, Massachusetts. 1998.

13. Montgomery, D. C. <u>Design and Analysis of Experiments</u>. Fifth Edition. John Wiley & Sons, Inc. New York, New York. 2001.

14. Anderson, R. M. Relationship Between Superpave Gyratory Compaction Properties on the Rutting Potential of Asphalt Mixes. Presented at the Annual Meeting of the Association of Asphalt Paving Technologists. Colorado Springs, Colorado. March 2002 (to be published in Vol. 71).

APPENDIX A

Raw Workability Data From Task 4

Table A.1. Test Results for 12.5 mm NMAS Granite Mixes

					Rep1				Rep2				
Aggregate	NMAS	Grad.	Binder	Temp	Constant	X1	R^2	Pred.	Constant	X1	R^2	Pred.	Avg. Pred
Granite	12.5	ARZ	64	120	11.8756	-1.28443	79.8	307	11.405	-1.19111	72.7	300	303
Granite	12.5	ARZ	64	130	11.8756	-1.28443	79.8	277	11.405	-1.19111	72.7	272	275
Granite	12.5	ARZ	64	140	11.8756	-1.28443	79.8	252	11.405	-1.19111	72.7	249	251
Granite	12.5	ARZ	64	150	11.8756	-1.28443	79.8	230	11.405	-1.19111	72.7	230	230
Granite	12.5	ARZ	64	160	11.8756	-1.28443	79.8	212	11.405	-1.19111	72.7	213	212
Granite	12.5	ARZ	64	170	11.8756	-1.28443	79.8	196	11.405	-1.19111	72.7	198	197
Granite	12.5	ARZ	70	120	13.0608	-1.52581	77.8	316	12.1982	-1.34842	78.3	312	314
Granite	12.5	ARZ	70	130	13.0608	-1.52581	77.8	280	12.1982	-1.34842	78.3	280	280
Granite	12.5	ARZ	70	140	13.0608	-1.52581	77.8	250	12.1982	-1.34842	78.3	253	252
Granite	12.5	ARZ	70	150	13.0608	-1.52581	77.8	225	12.1982	-1.34842	78.3	231	228
Granite	12.5	ARZ	70	160	13.0608	-1.52581	77.8	204	12.1982	-1.34842	78.3	212	208
Granite	12.5	ARZ	70	170	13.0608	-1.52581	77.8	186	12.1982	-1.34842	78.3	195	190
Granite	12.5	ARZ	76	120	13.4793	-1.56552	82.1	397	11.8332	-1.21061	73.0	419	408
Granite	12.5	ARZ	76	130	13.4793	-1.56552	82.1	350	11.8332	-1.21061	73.0	380	365
Granite	12.5	ARZ	76	140	13.4793	-1.56552	82.1	312	11.8332	-1.21061	73.0	348	330
Granite	12.5	ARZ	76	150	13.4793	-1.56552	82.1	280	11.8332	-1.21061	73.0	320	300
Granite	12.5	ARZ	76	160	13.4793	-1.56552	82.1	253	11.8332	-1.21061	73.0	296	274
Granite	12.5	ARZ	76	170	13.4793	-1.56552	82.1	230	11.8332	-1.21061	73.0	275	252
Granite	12.5	BRZ	64	120	11.6313	-1.24139	66.7	295	11.1914	-1.14227	62.1	306	301
Granite	12.5	BRZ	64	130	11.6313	-1.24139	66.7	267	11.1914	-1.14227	62.1	279	273
Granite	12.5	BRZ	64	140	11.6313	-1.24139	66.7	244	11.1914	-1.14227	62.1	256	250
Granite	12.5	BRZ	64	150	11.6313	-1.24139	66.7	224	11.1914	-1.14227	62.1	237	230
Granite	12.5	BRZ	64	160	11.6313	-1.24139	66.7	207	11.1914	-1.14227	62.1	220	213
Granite	12.5	BRZ	64	170	11.6313	-1.24139	66.7	192	11.1914	-1.14227	62.1	205	199
Granite	12.5	BRZ	70	120	13.3029	-1.58013	81.5	310	11.893	-1.31074	72.7	275	293
Granite	12.5	BRZ	70	130	13.3029	-1.58013	81.5	274	11.893	-1.31074	72.7	248	261
Granite	12.5	BRZ	70	140	13.3029	-1.58013	81.5	243	11.893	-1.31074	72.7	225	234
Granite	12.5	BRZ	70	150	13.3029	-1.58013	81.5	218	11.893	-1.31074	72.7	205	212
Granite	12.5	BRZ	70	160	13.3029	-1.58013	81.5	197	11.893	-1.31074	72.7	189	193
Granite	12.5	BRZ	70	170	13.3029	-1.58013	81.5	179	11.893	-1.31074	72.7	174	177
Granite	12.5	BRZ	76	120	13.664	-1.57859	76.5	449	15.4536	-1.93238	87.9	494	471
Granite	12.5	BRZ	76	130	13.664	-1.57859	76.5	396	15.4536	-1.93238	87.9	423	409
Granite	12.5	BRZ	76	140	13.664	-1.57859	76.5	352	15.4536	-1.93238	87.9	367	359
Granite	12.5	BRZ	76	150	13.664	-1.57859	76.5	316	15.4536	-1.93238	87.9	321	318
Granite	12.5	BRZ	76	160	13.664	-1.57859	76.5	285	15.4536	-1.93238	87.9	283	284
Granite	12.5	BRZ	76	170	13.664	-1.57859	76.5	259	15.4536	-1.93238	87.9	252	255

Table A.2. Test Results for 19.0 mm NMAS Granite Mixes

					Rep1				Rep2				
Aggregate	NMAS	Grad.	Binder	Temp	Constant	X1	R^2	Pred.	Constant	X1	R^2	Pred.	Avg. Pred
Granite	19	ARZ	64	120	11.2601	-1.12192	53.7	361	9.9522	-0.85896	32.9	344	352
Granite	19	ARZ	64	130	11.2601	-1.12192	53.7	330	9.9522	-0.85896	32.9	321	325
Granite	19	ARZ	64	140	11.2601	-1.12192	53.7	304	9.9522	-0.85896	32.9	301	302
Granite	19	ARZ	64	150	11.2601	-1.12192	53.7	281	9.9522	-0.85896	32.9	284	282
Granite	19	ARZ	64	160	11.2601	-1.12192	53.7	261	9.9522	-0.85896	32.9	268	265
Granite	19	ARZ	64	170	11.2601	-1.12192	53.7	244	9.9522	-0.85896	32.9	255	250
Granite	19	ARZ	70	120	12.4413	-1.37664	66.8	347	12.2006	-1.33797	61.4	329	338
Granite	19	ARZ	70	130	12.4413	-1.37664	66.8	311	12.2006	-1.33797	61.4	295	303
Granite	19	ARZ	70	140	12.4413	-1.37664	66.8	281	12.2006	-1.33797	61.4	267	274
Granite	19	ARZ	70	150	12.4413	-1.37664	66.8	256	12.2006	-1.33797	61.4	244	250
Granite	19	ARZ	70	160	12.4413	-1.37664	66.8	234	12.2006	-1.33797	61.4	224	229
Granite	19	ARZ	70	170	12.4413	-1.37664	66.8	215	12.2006	-1.33797	61.4	206	211
Granite	19	ARZ	76	120	9.96451	-0.82267	33.7	414	11.2846	-1.09825	50.2	414	414
Granite	19	ARZ	76	130	9.96451	-0.82267	33.7	388	11.2846	-1.09825	50.2	379	384
Granite	19	ARZ	76	140	9.96451	-0.82267	33.7	365	11.2846	-1.09825	50.2	350	357
Granite	19	ARZ	76	150	9.96451	-0.82267	33.7	345	11.2846	-1.09825	50.2	324	334
Granite	19	ARZ	76	160	9.96451	-0.82267	33.7	327	11.2846	-1.09825	50.2	302	314
Granite	19	ARZ	76	170	9.96451	-0.82267	33.7	311	11.2846	-1.09825	50.2	283	297
Granite	19	BRZ	64	120	11.4369	-1.16053	52.0	358	12.3719	-1.37731	64.3	323	341
Granite	19	BRZ	64	130	11.4369	-1.16053	52.0	326	12.3719	-1.37731	64.3	289	308
Granite	19	BRZ	64	140	11.4369	-1.16053	52.0	299	12.3719	-1.37731	64.3	261	280
Granite	19	BRZ	64	150	11.4369	-1.16053	52.0	276	12.3719	-1.37731	64.3	238	257
Granite	19	BRZ	64	160	11.4369	-1.16053	52.0	256	12.3719	-1.37731	64.3	217	237
Granite	19	BRZ	64	170	11.4369	-1.16053	52.0	239	12.3719	-1.37731	64.3	200	220
Granite	19	BRZ	70	120	10.9478	-1.09109	41.4	306	12.4963	-1.39241	62.7	340	323
Granite	19	BRZ	70	130	10.9478	-1.09109	41.4	281	12.4963	-1.39241	62.7	305	293
Granite	19	BRZ	70	140	10.9478	-1.09109	41.4	259	12.4963	-1.39241	62.7	275	267
Granite	19	BRZ	70	150	10.9478	-1.09109	41.4	240	12.4963	-1.39241	62.7	249	245
Granite	19	BRZ	70	160	10.9478	-1.09109	41.4	224	12.4963	-1.39241	62.7	228	226
Granite	19	BRZ	70	170	10.9478	-1.09109	41.4	209	12.4963	-1.39241	62.7	210	209
Granite	19	BRZ	76	120	13.2362	-1.52643	71.1	376	12.4413	-1.36176	63.2	373	374
Granite	19	BRZ	76	130	13.2362	-1.52643	71.1	332	12.4413	-1.36176	63.2	335	333
Granite	19	BRZ	76	140	13.2362	-1.52643	71.1	297	12.4413	-1.36176	63.2	302	300
Granite	19	BRZ	76	150	13.2362	-1.52643	71.1	267	12.4413	-1.36176	63.2	275	271
Granite	19	BRZ	76	160	13.2362	-1.52643	71.1	242	12.4413	-1.36176	63.2	252	247
Granite	19	BRZ	76	170	13.2362	-1.52643	71.1	221	12.4413	-1.36176	63.2	232	226

Table A.3. Test Results for 12.5 mm NMAS Crushed Gravel Mixes

					Rep1				Rep2				
Aggregate	NMAS	Grad.	Binder	Temp	Constant	X1	R^2	Pred.	Constant	X1	R^2	Pred.	Avg. Pred
Cr. Gravel	12.5	ARZ	64	120	10.6278	-1.08866	63.1	225	10.9686	-1.15742	74.4	228	226
Cr. Gravel	12.5	ARZ	64	130	10.6278	-1.08866	63.1	206	10.9686	-1.15742	74.4	207	207
Cr. Gravel	12.5	ARZ	64	140	10.6278	-1.08866	63.1	190	10.9686	-1.15742	74.4	190	190
Cr. Gravel	12.5	ARZ	64	150	10.6278	-1.08866	63.1	176	10.9686	-1.15742	74.4	176	176
Cr. Gravel	12.5	ARZ	64	160	10.6278	-1.08866	63.1	164	10.9686	-1.15742	74.4	163	164
Cr. Gravel	12.5	ARZ	64	170	10.6278	-1.08866	63.1	154	10.9686	-1.15742	74.4	152	153
Cr. Gravel	12.5	ARZ	70	120	11.5368	-1.27062	77.8	234	12.105	-1.37646	88.1	248	241
Cr. Gravel	12.5	ARZ	70	130	11.5368	-1.27062	77.8	211	12.105	-1.37646	88.1	223	217
Cr. Gravel	12.5	ARZ	70	140	11.5368	-1.27062	77.8	192	12.105	-1.37646	88.1	201	197
Cr. Gravel	12.5	ARZ	70	150	11.5368	-1.27062	77.8	176	12.105	-1.37646	88.1	183	179
Cr. Gravel	12.5	ARZ	70	160	11.5368	-1.27062	77.8	162	12.105	-1.37646	88.1	167	165
Cr. Gravel	12.5	ARZ	70	170	11.5368	-1.27062	77.8	150	12.105	-1.37646	88.1	154	152
Cr. Gravel	12.5	ARZ	76	120	12.2599	-1.37034	75.6	299	11.3644	-1.18049	68.6	303	301
Cr. Gravel	12.5	ARZ	76	130	12.2599	-1.37034	75.6	268	11.3644	-1.18049	68.6	275	272
Cr. Gravel	12.5	ARZ	76	140	12.2599	-1.37034	75.6	242	11.3644	-1.18049	68.6	252	247
Cr. Gravel	12.5	ARZ	76	150	12.2599	-1.37034	75.6	220	11.3644	-1.18049	68.6	233	226
Cr. Gravel	12.5	ARZ	76	160	12.2599	-1.37034	75.6	201	11.3644	-1.18049	68.6	216	208
Cr. Gravel	12.5	ARZ	76	170	12.2599	-1.37034	75.6	185	11.3644	-1.18049	68.6	201	193
Cr. Gravel	12.5	BRZ	64	120	10.5387	-1.08224	66.7	212	10.088	-0.96564	64.2	236	224
Cr. Gravel	12.5	BRZ	64	130	10.5387	-1.08224	66.7	195	10.088	-0.96564	64.2	219	207
Cr. Gravel	12.5	BRZ	64	140	10.5387	-1.08224	66.7	180	10.088	-0.96564	64.2	204	192
Cr. Gravel	12.5	BRZ	64	150	10.5387	-1.08224	66.7	167	10.088	-0.96564	64.2	190	179
Cr. Gravel	12.5	BRZ	64	160	10.5387	-1.08224	66.7	155	10.088	-0.96564	64.2	179	167
Cr. Gravel	12.5	BRZ	64	170	10.5387	-1.08224	66.7	146	10.088	-0.96564	64.2	169	157
Cr. Gravel	12.5	BRZ	70	120	12.2628	-1.39477	92.2	266	11.5555	-1.2546	85	257	262
Cr. Gravel	12.5	BRZ	70	130	12.2628	-1.39477	92.2	238	11.5555	-1.2546	85	232	235
Cr. Gravel	12.5	BRZ	70	140	12.2628	-1.39477	92.2	215	11.5555	-1.2546	85	212	213
Cr. Gravel	12.5	BRZ	70	150	12.2628	-1.39477	92.2	195	11.5555	-1.2546	85	194	195
Cr. Gravel	12.5	BRZ	70	160	12.2628	-1.39477	92.2	178	11.5555	-1.2546	85	179	179
Cr. Gravel	12.5	BRZ	70	170	12.2628	-1.39477	92.2	164	11.5555	-1.2546	85	166	165
Cr. Gravel	12.5	BRZ	76	120	14.7576	-1.84518	87.2	374	12.42	-1.38405	78.1	328	351
Cr. Gravel	12.5	BRZ	76	130	14.7576	-1.84518	87.2	323	12.42	-1.38405	78.1	294	308
Cr. Gravel	12.5	BRZ	76	140	14.7576	-1.84518	87.2	281	12.42	-1.38405	78.1	265	273
Cr. Gravel	12.5	BRZ	76	150	14.7576	-1.84518	87.2	248	12.42	-1.38405	78.1	241	244
Cr. Gravel	12.5	BRZ	76	160	14.7576	-1.84518	87.2	220	12.42	-1.38405	78.1	220	220
Cr. Gravel	12.5	BRZ	76	170	14.7576	-1.84518	87.2	197	12.42	-1.38405	78.1	203	200

Table A.4. Test Results for 19.0 mm NMAS Crushed Gravel Mixes

					Rep1				Rep2				
Aggregate	NMAS	Grad.	Binder	Temp	Constant	X1	R^2	Pred.	Constant	X1	R^2	Pred.	Avg. Pred
Cr. Gravel	19	ARZ	64	120	12.9375	-1.49444	75.2	325	11.3957	-1.21644	57.8	263	294
Cr. Gravel	19	ARZ	64	130	12.9375	-1.49444	75.2	288	11.3957	-1.21644	57.8	239	263
Cr. Gravel	19	ARZ	64	140	12.9375	-1.49444	75.2	258	11.3957	-1.21644	57.8	218	238
Cr. Gravel	19	ARZ	64	150	12.9375	-1.49444	75.2	233	11.3957	-1.21644	57.8	200	217
Cr. Gravel	19	ARZ	64	160	12.9375	-1.49444	75.2	211	11.3957	-1.21644	57.8	185	198
Cr. Gravel	19	ARZ	64	170	12.9375	-1.49444	75.2	193	11.3957	-1.21644	57.8	172	183
Cr. Gravel	19	ARZ	70	120	12.0667	-1.36168	69.5	257	10.5536	-1.03936	60.2	264	261
Cr. Gravel	19	ARZ	70	130	12.0667	-1.36168	69.5	230	10.5536	-1.03936	60.2	243	237
Cr. Gravel	19	ARZ	70	140	12.0667	-1.36168	69.5	208	10.5536	-1.03936	60.2	225	217
Cr. Gravel	19	ARZ	70	150	12.0667	-1.36168	69.5	189	10.5536	-1.03936	60.2	210	200
Cr. Gravel	19	ARZ	70	160	12.0667	-1.36168	69.5	173	10.5536	-1.03936	60.2	196	185
Cr. Gravel	19	ARZ	70	170	12.0667	-1.36168	69.5	160	10.5536	-1.03936	60.2	184	172
Cr. Gravel	19	ARZ	76	120	12.4267	-1.38696	53.6	326	11.4347	-1.18236	50.1	322	324
Cr. Gravel	19	ARZ	76	130	12.4267	-1.38696	53.6	292	11.4347	-1.18236	50.1	293	292
Cr. Gravel	19	ARZ	76	140	12.4267	-1.38696	53.6	263	11.4347	-1.18236	50.1	268	266
Cr. Gravel	19	ARZ	76	150	12.4267	-1.38696	53.6	239	11.4347	-1.18236	50.1	247	243
Cr. Gravel	19	ARZ	76	160	12.4267	-1.38696	53.6	219	11.4347	-1.18236	50.1	229	224
Cr. Gravel	19	ARZ	76	170	12.4267	-1.38696	53.6	201	11.4347	-1.18236	50.1	213	207
Cr. Gravel	19	BRZ	64	120	9.9063	-0.92213	36.8	243	9.91014	-0.91413	47.4	253	248
Cr. Gravel	19	BRZ	64	130	9.9063	-0.92213	36.8	225	9.91014	-0.91413	47.4	235	230
Cr. Gravel	19	BRZ	64	140	9.9063	-0.92213	36.8	210	9.91014	-0.91413	47.4	220	215
Cr. Gravel	19	BRZ	64	150	9.9063	-0.92213	36.8	198	9.91014	-0.91413	47.4	206	202
Cr. Gravel	19	BRZ	64	160	9.9063	-0.92213	36.8	186	9.91014	-0.91413	47.4	195	190
Cr. Gravel	19	BRZ	64	170	9.9063	-0.92213	36.8	176	9.91014	-0.91413	47.4	184	180
Cr. Gravel	19	BRZ	70	120	13.7102	-1.65964	82.3	319	11.8181	-1.30625	63.2	261	290
Cr. Gravel	19	BRZ	70	130	13.7102	-1.65964	82.3	279	11.8181	-1.30625	63.2	235	257
Cr. Gravel	19	BRZ	70	140	13.7102	-1.65964	82.3	247	11.8181	-1.30625	63.2	213	230
Cr. Gravel	19	BRZ	70	150	13.7102	-1.65964	82.3	220	11.8181	-1.30625	63.2	195	208
Cr. Gravel	19	BRZ	70	160	13.7102	-1.65964	82.3	198	11.8181	-1.30625	63.2	179	189
Cr. Gravel	19	BRZ	70	170	13.7102	-1.65964	82.3	179	11.8181	-1.30625	63.2	166	172
Cr. Gravel	19	BRZ	76	120	13.7426	-1.63308	72.4	374	13.8285	-1.65592	68.8	365	370
Cr. Gravel	19	BRZ	76	130	13.7426	-1.63308	72.4	328	13.8285	-1.65592	68.8	320	324
Cr. Gravel	19	BRZ	76	140	13.7426	-1.63308	72.4	291	13.8285	-1.65592	68.8	283	287
Cr. Gravel	19	BRZ	76	150	13.7426	-1.63308	72.4	260	13.8285	-1.65592	68.8	252	256
Cr. Gravel	19	BRZ	76	160	13.7426	-1.63308	72.4	234	13.8285	-1.65592	68.8	227	230
Cr. Gravel	19	BRZ	76	170	13.7426	-1.63308	72.4	212	13.8285	-1.65592	68.8	205	208

Table A.5. Test Results for 12.5 mm NMAS Limestone Mixes

Aggregate	NMAS	Gradation	Binder	Temp	Rep1 Constant	Rep1 X1	Rep1 R^2	Rep1 Pred.	Rep2 Constant	Rep2 X1	Rep2 R^2	Rep2 Pred.	Avg. Pred
Limestone	12.5	ARZ	64	120	10.7273	-1.0624	66.3	282	11.0541	-1.14848	80.2	259	270
Limestone	12.5	ARZ	64	130	10.7273	-1.0624	66.3	259	11.0541	-1.14848	80.2	236	247
Limestone	12.5	ARZ	64	140	10.7273	-1.0624	66.3	239	11.0541	-1.14848	80.2	217	228
Limestone	12.5	ARZ	64	150	10.7273	-1.0624	66.3	222	11.0541	-1.14848	80.2	200	211
Limestone	12.5	ARZ	64	160	10.7273	-1.0624	66.3	208	11.0541	-1.14848	80.2	186	197
Limestone	12.5	ARZ	64	170	10.7273	-1.0624	66.3	195	11.0541	-1.14848	80.2	173	184
Limestone	12.5	ARZ	70	120	10.3297	-0.97962	69.1	281	11.6742	-1.26772	81.9	272	277
Limestone	12.5	ARZ	70	130	10.3297	-0.97962	69.1	260	11.6742	-1.26772	81.9	246	253
Limestone	12.5	ARZ	70	140	10.3297	-0.97962	69.1	242	11.6742	-1.26772	81.9	224	233
Limestone	12.5	ARZ	70	150	10.3297	-0.97962	69.1	226	11.6742	-1.26772	81.9	205	215
Limestone	12.5	ARZ	70	160	10.3297	-0.97962	69.1	212	11.6742	-1.26772	81.9	189	201
Limestone	12.5	ARZ	70	170	10.3297	-0.97962	69.1	200	11.6742	-1.26772	81.9	175	187
Limestone	12.5	ARZ	76	120	11.6086	-1.17977	72.4	388	11.832	-1.25063	70.4	345	367
Limestone	12.5	ARZ	76	130	11.6086	-1.17977	72.4	353	11.832	-1.25063	70.4	312	333
Limestone	12.5	ARZ	76	140	11.6086	-1.17977	72.4	323	11.832	-1.25063	70.4	285	304
Limestone	12.5	ARZ	76	150	11.6086	-1.17977	72.4	298	11.832	-1.25063	70.4	261	280
Limestone	12.5	ARZ	76	160	11.6086	-1.17977	72.4	276	11.832	-1.25063	70.4	241	259
Limestone	12.5	ARZ	76	170	11.6086	-1.17977	72.4	257	11.832	-1.25063	70.4	223	240
Limestone	12.5	BRZ	64	120	11.5382	-1.23053	69.4	283	12.119	-1.35173	74.9	284	284
Limestone	12.5	BRZ	64	130	11.5382	-1.23053	69.4	257	12.119	-1.35173	74.9	255	256
Limestone	12.5	BRZ	64	140	11.5382	-1.23053	69.4	234	12.119	-1.35173	74.9	230	232
Limestone	12.5	BRZ	64	150	11.5382	-1.23053	69.4	215	12.119	-1.35173	74.9	210	213
Limestone	12.5	BRZ	64	160	11.5382	-1.23053	69.4	199	12.119	-1.35173	74.9	192	196
Limestone	12.5	BRZ	64	170	11.5382	-1.23053	69.4	185	12.119	-1.35173	74.9	177	181
Limestone	12.5	BRZ	70	120	14.3567	-1.7952	86.8	318	14.8167	-1.8812	89.4	334	326
Limestone	12.5	BRZ	70	130	14.3567	-1.7952	86.8	275	14.8167	-1.8812	89.4	287	281
Limestone	12.5	BRZ	70	140	14.3567	-1.7952	86.8	241	14.8167	-1.8812	89.4	250	245
Limestone	12.5	BRZ	70	150	14.3567	-1.7952	86.8	213	14.8167	-1.8812	89.4	219	216
Limestone	12.5	BRZ	70	160	14.3567	-1.7952	86.8	190	14.8167	-1.8812	89.4	194	192
Limestone	12.5	BRZ	70	170	14.3567	-1.7952	86.8	170	14.8167	-1.8812	89.4	173	172
Limestone	12.5	BRZ	76	120	16.9174	-2.23833	89.1	493	15.5468	-1.96695	86.8	459	476
Limestone	12.5	BRZ	76	130	16.9174	-2.23833	89.1	413	15.5468	-1.96695	86.8	393	403
Limestone	12.5	BRZ	76	140	16.9174	-2.23833	89.1	349	15.5468	-1.96695	86.8	339	344
Limestone	12.5	BRZ	76	150	16.9174	-2.23833	89.1	299	15.5468	-1.96695	86.8	296	298
Limestone	12.5	BRZ	76	160	16.9174	-2.23833	89.1	259	15.5468	-1.96695	86.8	261	260
Limestone	12.5	BRZ	76	170	16.9174	-2.23833	89.1	226	15.5468	-1.96695	86.8	232	229

Table A.6. Test Results for 19.0 mm NMAS Limestone Mixes

					Rep1				Rep2				
Aggregate	NMAS	Gradation	Binder	Temp	Constant	X1	R^2	Pred.	Constant	X1	R^2	Pred.	Avg. Pred
Limestone	19	ARZ	64	120	11.2917	-1.14884	51.2	328	11.623	-1.19864	59.6	359	343
Limestone	19	ARZ	64	130	11.2917	-1.14884	51.2	299	11.623	-1.19864	59.6	327	313
Limestone	19	ARZ	64	140	11.2917	-1.14884	51.2	274	11.623	-1.19864	59.6	299	287
Limestone	19	ARZ	64	150	11.2917	-1.14884	51.2	253	11.623	-1.19864	59.6	275	264
Limestone	19	ARZ	64	160	11.2917	-1.14884	51.2	235	11.623	-1.19864	59.6	255	245
Limestone	19	ARZ	64	170	11.2917	-1.14884	51.2	220	11.623	-1.19864	59.6	237	228
Limestone	19	ARZ	70	120	11.8108	-1.24244	46.2	352	11.6253	-1.22479	47.1	318	335
Limestone	19	ARZ	70	130	11.8108	-1.24244	46.2	318	11.6253	-1.22479	47.1	288	303
Limestone	19	ARZ	70	140	11.8108	-1.24244	46.2	290	11.6253	-1.22479	47.1	263	277
Limestone	19	ARZ	70	150	11.8108	-1.24244	46.2	267	11.6253	-1.22479	47.1	242	254
Limestone	19	ARZ	70	160	11.8108	-1.24244	46.2	246	11.6253	-1.22479	47.1	223	235
Limestone	19	ARZ	70	170	11.8108	-1.24244	46.2	228	11.6253	-1.22479	47.1	207	218
Limestone	19	ARZ	76	120	10.1296	-0.86895	25.2	391	9.8751	-0.81251	16.7	398	394
Limestone	19	ARZ	76	130	10.1296	-0.86895	25.2	365	9.8751	-0.81251	16.7	372	369
Limestone	19	ARZ	76	140	10.1296	-0.86895	25.2	342	9.8751	-0.81251	16.7	351	346
Limestone	19	ARZ	76	150	10.1296	-0.86895	25.2	322	9.8751	-0.81251	16.7	332	327
Limestone	19	ARZ	76	160	10.1296	-0.86895	25.2	305	9.8751	-0.81251	16.7	315	310
Limestone	19	ARZ	76	170	10.1296	-0.86895	25.2	289	9.8751	-0.81251	16.7	300	294
Limestone	19	BRZ	64	120	13.2934	-1.57209	68.6	320	13.7083	-1.67248	75.6	299	309
Limestone	19	BRZ	64	130	13.2934	-1.57209	68.6	282	13.7083	-1.67248	75.6	262	272
Limestone	19	BRZ	64	140	13.2934	-1.57209	68.6	251	13.7083	-1.67248	75.6	231	241
Limestone	19	BRZ	64	150	13.2934	-1.57209	68.6	225	13.7083	-1.67248	75.6	206	216
Limestone	19	BRZ	64	160	13.2934	-1.57209	68.6	203	13.7083	-1.67248	75.6	185	194
Limestone	19	BRZ	64	170	13.2934	-1.57209	68.6	185	13.7083	-1.67248	75.6	167	176
Limestone	19	BRZ	70	120	15.392	-1.96915	78.6	389	15.7203	-2.04932	79.3	368	379
Limestone	19	BRZ	70	130	15.392	-1.96915	78.6	333	15.7203	-2.04932	79.3	313	323
Limestone	19	BRZ	70	140	15.392	-1.96915	78.6	287	15.7203	-2.04932	79.3	269	278
Limestone	19	BRZ	70	150	15.392	-1.96915	78.6	251	15.7203	-2.04932	79.3	233	242
Limestone	19	BRZ	70	160	15.392	-1.96915	78.6	221	15.7203	-2.04932	79.3	204	213
Limestone	19	BRZ	70	170	15.392	-1.96915	78.6	196	15.7203	-2.04932	79.3	180	188
Limestone	19	BRZ	76	120	18.0066	-2.4438	82.6	548	18.839	-2.61294	84.8	561	555
Limestone	19	BRZ	76	130	18.0066	-2.4438	82.6	451	18.839	-2.61294	84.8	455	453
Limestone	19	BRZ	76	140	18.0066	-2.4438	82.6	376	18.839	-2.61294	84.8	375	376
Limestone	19	BRZ	76	150	18.0066	-2.4438	82.6	318	18.839	-2.61294	84.8	313	315
Limestone	19	BRZ	76	160	18.0066	-2.4438	82.6	271	18.839	-2.61294	84.8	265	268
Limestone	19	BRZ	76	170	18.0066	-2.4438	82.6	234	18.839	-2.61294	84.8	226	230